universität wien

DIPLOMARBEIT

Titel der Diplomarbeit

Assessment of Therapeutic Drug Efficacy
in the Epithelial to Mesenchymal Transition of Human Liver Cancer

angestrebter akademischer Grad

Magistra der Naturwissenschaften (Mag. rer.nat.)

Verfasserin:	Sabine Mall
Studienrichtung:	Molekulare Biologie (A490)
Betreuerin / Betreuer:	A.o. univ. Prof. Dr. Wolfgang Mikulits

Wien, am 05.07.2010

Für meine Familie und Raini

Kannst du einen Stern berühren, fragte man es. -

Ja, sagte das Kind, neigte sich und berührte die Erde.

Hugo von Hofmannsthal

Table of contents:

1. Summary/Zusammenfassung

1.1. Summary

Hepatocellular carcinoma (HCC) is the sixth most common cancer worldwide and the incidence is still increasing. The epithelial to mesenchymal transition (EMT) of malignant hepatocytes in HCC is considered as a major cause of liver cancer progression and metastasis.

In this study we aimed to establish a human cellular model of HCC to investigate the molecular mechanisms of EMT and to examine the efficacy of anti-cancer agents in this process.Two liver cell lines were established from one HCC patient showing either an epithelial or mesenchymal phenotype. Immunofluorescence analysis confirmed the distinct epithelial and mesenchymal characteristics of HCC cells. Most remarkably, mesenchymal HCC cells showed enhanced migration and invasion *in vitro*. Comparative genomic hybridization and short tandem repeat analysis indicated a unique cellular origin of both cell types, suggesting that mesenchymal cells derived from epithelial hepatocytes via EMT *in vivo*. Loss of epithelial as well as gain of mesenchymal markers analyzed by whole genome expression profiling verified EMT. Interestingly, methylation-specific PCR analysis revealed epigenetic upregulation of secreted protein, acidic, rich in cystein (SPARC) in mesenchymal cells via promoter demethylation. Upon drug exposure, mesenchymal HCC cells showed a higher resistance to the targeted therapeutic agents sorafenib and erlotinib as compared to epithelial HCC cells, which were slightly more resistant to cytostatic drugs. Combination of doxorubicin and sorafenib caused an increased susceptibility of both cell lines to cytostatic effects resulting in an equalization of IC_{50} values, thus showing an effective treatment to target both, epithelial and mesenchymal cells.

In conclusion, we established a unique EMT model of human HCC for pre-clinical studies which allows studying drug efficacy during HCC progression including the assessment of synergistic anti-cancer drug profiles.

1.2. Zusammenfassung

Das hepatozelluläre Karzinom ist die sechst häufigste Krebserkrankung weltweit, dessen Inzidenz nach wie vor steigend ist. Die epitheliale zur mesenchymalen Transition (EMT), ein Prozess bei dem epitheliale Zellen ihre typische Organisation verlieren und dadurch in das umliegende Gewebe invadieren können, wurde als eine Hauptursache der fortschreitenden Leberkrebserkrankung und deren Metastasierung identifiziert.

Ziel dieser experimentellen Studie war, ein humanes zelluläres Modell der EMT zu entwickeln, um einerseits molekulare Mechanismen der EMT zu identifizieren und andererseits die Effizienz antitumoraler Medikamente in diesem Prozess zu untersuchen. Dafür wurden zwei Leber-Zelllinien, welche einen epithelialen beziehungsweise einen mesenchymalen Phänotyp aufweisen, aus dem Tumor eines HCC Patienten isoliert. Die Immunfluoreszenzanalyse bestätigte die epithelialen und mesenchymalen Charakteristika dieser HCC Zelllinien. Weiters konnten wir zeigen, dass die mesenchymalen HCC Zellen, im Vergleich zu den epithelialen, eine höhere Migration und Invasion *in vitro* aufweisen. Die chromosomale Analyse mittels vergleichender genomischen Hybridisierung und eine 'Short Tandem Repeat' Analyse bestätigten, dass beide Zelltypen ursprünglich aus einer Zelle entstanden sind. Dies zeigt damit eindeutig, dass sich die mesenchymalen Zellen durch eine EMT *in vivo* aus den epithelialen Zellen entwickelt haben. Durch die Expressionsanalyse des gesamten Transkriptoms konnte der Verlust von epithelialen und der Erwerb von mesenchymalen Markern nachgewiesen werden, wodurch eine EMT bestätigt wurde. Eine methylierungsspezifische Polymerase- Kettenreaktion (PCR) ergab weiters, dass das Protein 'Secreted Protein, Acidic, Rich in Cystein' (SPARC), das in den mesenchymalen HCC Zellen stark überexprimiert ist, durch Demethylierung seines Promotors epigenetisch reguliert wird. Ebenso konnten wir zeigen, dass mesenchymale HCC Zellen im Vergleich zu den epithelialen HCC Zellen eine höhere Resistenz gegen zielgerichte Therapien wie Sorafenib und Erlotinib

aufweisen, wohingegen epitheliale HCC Zellen stärker resistent gegen zytostatische Medikamente sind. Die Kombination von Doxorubicin und Sorafenib verursacht eine erhöhte Empfindlichkeit von beiden Zelllinien, was dazu führt, dass sich die maximalen mittleren inhibitorischen Konzentrationen (IC_{50}) einander angleichen. Diese Kombination ist folglich eine effiziente Behandlung um beide, eptiheliale als auch mesenchymale Hepatomzellen erfolgreich zu eliminieren.

Zusammenfassend konnten wir ein einzigartiges EMT Modell des humanen HCCs entwickeln, das in präklinischen Studien eingesetzt werden kann, um (i) die cytostatische Effizienz einer Substanz in vitro zu testen, (ii) ein Profil des Wirkstoffs mit dessen Auswirkung auf zelluläre Mechanismen zu erstellen und (iii) Synergismen mit weiteren Antikrebsmitteln zu identifizieren.

2. Introduction

2.1. Hepatocellular carcinoma - HCC

Hepatocellular carcinoma (HCC) is the sixth most common cancer worldwide (Parkin *et al.*, 2005) and the incidence is still increasing in Europe and the United States (El-Serag and Mason, 1999). The survival rates are 3% to 5% in the US and developing countries due to its very poor prognosis. Therefore, HCC is categorized as the third most common cause of death from cancer (Parkin *et al.*, 2005). HCC has well defined major risk factors including infections with hepatitis B or C (HBV or HCV), Aflatoxin B1 intoxication, and chronic alcohol abuse (El-Serag and Mason, 1999). The incidence of HCC varies geographically, corresponding to the distribution of risk factors worldwide. For example, HBV infection and Aflatoxin B1 intoxication from contaminated food are common in Asia and Africa. In contrast, the main risk factors in the Western World and Japan are HCV infections as well as alcohol abuse (El-Serag and Rudolph, 2007). These multiple factors contributing to HCC development might explain the complex molecular pathogenesis of this disease (Thorgeirsson and Grisham, 2002).

Development of HCC

Hepatocaricinogenesis is a multifactorial and multistep process that involves various genetic and epigenetic changes which finally lead to malignant transformation of hepatocytes (Blum and Spangenberg, 2007). 80% of all HCC cases develop from cirrhotic livers. This continuous damage and regeneration of hepatocytes in a context of inflammation, immune response or oxidative DNA damage leads to the development of hyperplastic nodules (Blum and Spangenberg, 2007), which represent a potential first step towards HCC (Figure 1). These lesions can progress to pre-malignant dysplastic nodules, surrounded by connective tissue. Finally, dysplastic nodules can evolve into HCC by addition of other genetic or epigenetic

changes. HCC can be classified into well, moderately or poor differentiated tumors, of which the latter represents the most malignant form of primary HCC (Figure 1; Farazi and DePinho, 2006). Further progression of the disease leads to vascular invasion which subsequently leads to intrahepatic dissemination of cancer cells. In advanced stages of HCC, tumor cells can invade into larger vessels, mostly into portal veins and finally circulate systemically through the blood stream and metastasize into distant organs (Schwartz *et al.*, 2007).

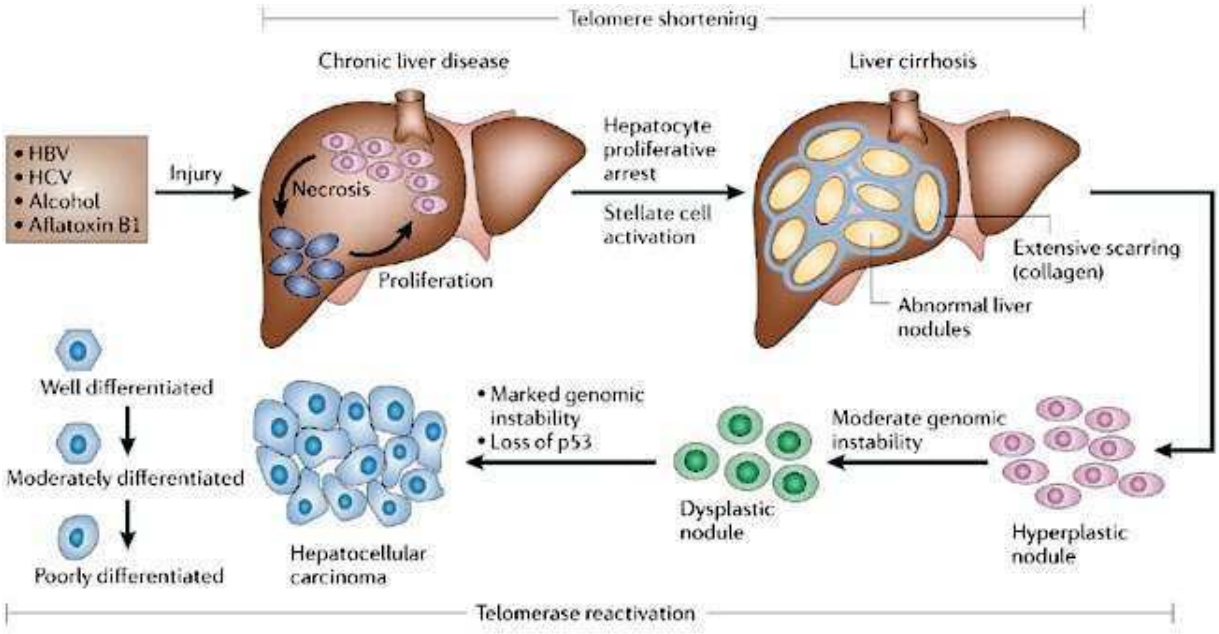

Figure 1. Pathogenesis of hepatocellular carcinoma (Farazi and DePinho, 2006). Continuous hepatic necrosis and regeneration in chronic liver disease leads to the development of abnormal liver nodules in a cirrhotic background. Pre-malignant hyperplastic nodules with increased genomic instability evolve into dysplastic cells, which can develop HCC after further genetic or epigenetic changes.

Molecular mechanisms of HCC

Several key mechanisms are involved in tumor formation and can be classified in six functional groups including self- sufficiency in growth signals, insensitivity to anti-growth signals, evasion of apoptosis, limitless replicative potential, sustained angiogenesis, and tumor invasion and metastasis (Figure 2; Hanahan and Weinberg, 2000).

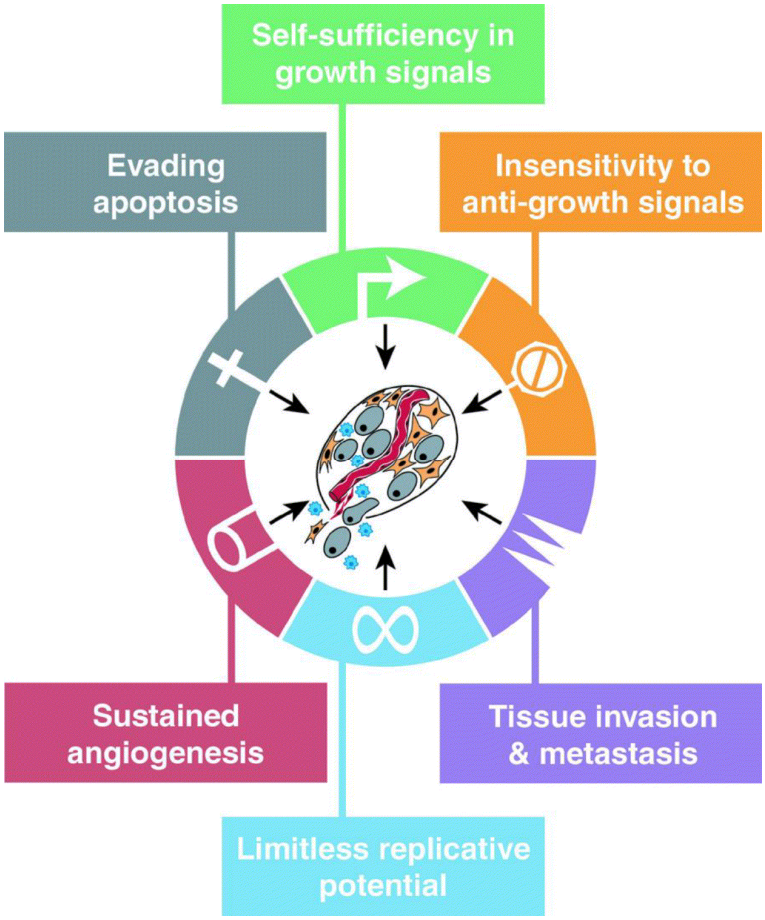

Figure 2. Acquired functions of cancer cells (Hanahan and Weinberg, 2000). During cancer development, most cancer cells gain a set of functional capabilities.

The genetic aberrations and signaling pathways involved in hepatocarcinogenesis are mostly depending on the various etiologies, but there are some common molecular changes in HCC development (Aravalli *et al.*, 2008; Farazi and DePinho, 2006):

1. Genetic aberrations: Overall, telomerase activity was found to be increased in the majority of HCCs (Farazi *et al.*, 2003). Several other genes were found to be frequently related to hepatocarcinogenesis of which the overexpression of c-myc and CCND1/Cyclin D1 as well as the mutation or deletion of tumor suppressor such as AXIN1, p53, CDH1/E-cadherin or PTEN are the most common ones (Minguez *et al.*, 2009).
2. Wnt/β-catenin pathway: This pathway was shown to be the most common disrupted pathway in HCC. It is involved in HCC arising from virus-infections and alcoholic liver cirrhosis (Aravalli *et al.*, 2008). Mutations in β-catenin or AXIN1, epigenetic silencing of E-cadherin or aberrant expression of Wnt/frizzeled receptors are the most causes for the activation of the Wnt/β-catenin pathway, which leads to the translocation of membrane-bound β-catenin into the nucleus where it acts as a transcriptional regulator of oncogenes such as c-myc and cyclin D1 (Minguez *et al.*, 2009).
3. p53 pathway: The tumor suppressor gene TP53 is inactivated in about half of all human tumors and in about 30%- 60% of HCC patients (Cha and Dematteo, 2005; Minguez *et al.*, 2009). Under physiological conditions, p53 suppresses cell replication and induces apoptosis (Kern *et al.*, 1992). The loss of p53 leads to an uncontrolled expansion of hepatocytes, chromosomal instability and initiation of HCC (El-Serag and Rudolph, 2007). Indeed, mutations in the TP53 were found to be associated with a higher chromosomal instability, poor differentiated tumors and poor prognosis of patients (Honda *et al.*, 1998; Laurent-Puig *et al.*, 2001). The p53 pathway can be affected at different levels in human HCC. Beside mutations in the p53 gene, microdeletions of $p14^{ARF}$ occur in 15%-20% of human HCC and overexpression of Mdm2 as well as Gankyrin, which inhibits the Retinoblastoma (Rb) - and p53- checkpoints, were observed in human HCCs (El-Serag and Rudolph, 2007).
4. The phosphoinositide 3-kinase (PI3K)/Akt/mammalian target of Rapamycin (mTOR) pathway is activated in 30-50% of all HCCs. It can be upregulated via abnormal activation

of tyrosine kinase receptors, including epidermal growth factor receptor (EGFR), vascular endothelial growth factor receptor (VEGFR), or platelet derived growth factor receptor (PDGFR). Alternatively, the loss of the tumor suppressor gene PTEN leads to the constitutive activation of PI3K (Villanueva *et al.*, 2008).

5. The Ras/Raf/Erk pathway is activated in nearly all advanced stages of liver cancer, mostly as a result of increased upstream signaling by epidermal growth factor (EGF), hepatocyte growth factor (HGF) or insuline like growth factor (IGF) (Calvisi *et al.*, 2006).
6. ErbB receptors belong to the receptor tyrosine kinase family and all four members (ERBB1-ERBB4) are found to be overexpressed in HCC. ERBB1, also kown as EGFR, and ERBB3 expression were found to correlate with higher aggressiveness of HCC (Farazi and DePinho, 2006; Ito *et al.*, 2001).
7. Vascular endothelial growth factor (VEGF), also known as vascular permeability factor, is known to play an important role in angiogenesis. HCC is a highly vascularized tumor, and angiogenesis plays an important role in its development and progression. On the one hand VEGF stimulates cell proliferation and thus, budding of new blood vessels around the growing tumor. On the other hand it facilitates cell migration during invasion via promotion of fibrin scaffolding (Kaseb *et al.*, 2009). VEGF was shown to be expressed in 63% of encapsulated, 78% of nonencapsulated HCCs and in 90% of HCCs with extrahepatic metastasis (Yao *et al.*, 2005). Another study showed a correlation of VEGF expression with vascular invasion, intrahepatic metastasis and shorter overall survival in HCC patients (Deli *et al.*, 2005).
8. The transforming growth factor beta (TGF-β) plays an important role in the suppression of hepatocyte proliferation under physiological conditions. However, its misregulation can result in tumorigenesis by promotion of cell invasion, downregulation of immune responses and modifications of the microenvironment (Massague, 2008). HCCs expressing late TGF-β responsive genes (anti-apoptotic and metastatic) demonstrate a

higher invasive phenotype and increased tumor recurrence compared to those showing an early TGF-β signature (tumor suppressive) (Coulouarn *et al.*, 2008).

Involvement of microRNAs in hepatocarcinogenesis

Different classes of noncoding RNAs have been found in mammalian cells, including small interfering RNAs (siRNA), small nucleolar RNAs (snRNA) and micro RNAs (miRNAs) (Aravalli *et al.*, 2008). miRNAs regulate the expression of their target mRNAs on a post-transcriptional level (Minguez *et al.*, 2009). The currently best known miRNA in the liver is miR-122, which was shown to target Cyclin G1 and to be associated with a poor prognosis in human HCC (Coulouarn *et al.*, 2009). MiR-21, which downregulates the expression of the tumor suppressor PTEN, was shown to be upregulated in HCC compared to nontumoral tissue (Meng *et al.*, 2007). Many other studies identified various deregulated miRNAs in HCC, i.e. the expression of miR-26 was found to be associated with poor prognosis in human HCC (Ji *et al.*, 2009). HCCs may have a distinct miRNA fingerprint according to risk factors, genetic alterations and malignancy of the tumor. Finding these relationships may provide new insights into miRNA deregulation in carcinogenesis. Thus, they may be promising diagnostic markers in hepatocarcinogenesis (Imbeaud *et al.*, 2010).

2.2. Classification of HCC

Molecular classification of HCC

In the past decades many studies on expression profiles of HCC were performed and different investigators tried to classify HCC based on its molecular expression signature. One recent study revealed by integration of genomic and molecular alterations five distinct classes of HCC (Chiang *et al.*, 2008). One is associated with mutations in β-catenin, indicating that alterations in the canonical Wnt signalling are involved. Another subtype revealed increased proliferation, chromosomal instability and showed a high phosphorlylation rate of insulin-like growth factor 1 receptor (IGF-1R), ribosomal protein (RP)S6 and Akt. Another distinct subgroup showed an upregulation of interferon (IFN) stimulated genes, including signal transducer and activator of transcription (STAT) 1. Furthermore, a newly defined subclass showed a strong association with polysomy of chromosome 7.

Another recent study, a meta-analysis of 9 different transcriptome-analyses revealed three distinct molecular subclasses of HCC (Figure 3; Hoshida *et al.*, 2009). The subclass S1 is associated with an invasive phenotype, poor survival of patients and activated Wnt- and TGF-β gene expression signature. The S2 subclass comprises tumors with a MYC and AKT activated signature and also correlates with poor survival. Subclass S3 tumors showed a hepatocyte-related gene expression and are associated with good survival of patients (Hoshida *et al.*, 2009).

These analyses may help to define a robust molecular classification of HCC (Imbeaud *et al.*), to identify new biomarkers for early detection of tumor progression and to unravel new targets for therapies (Chiang *et al.*, 2008).

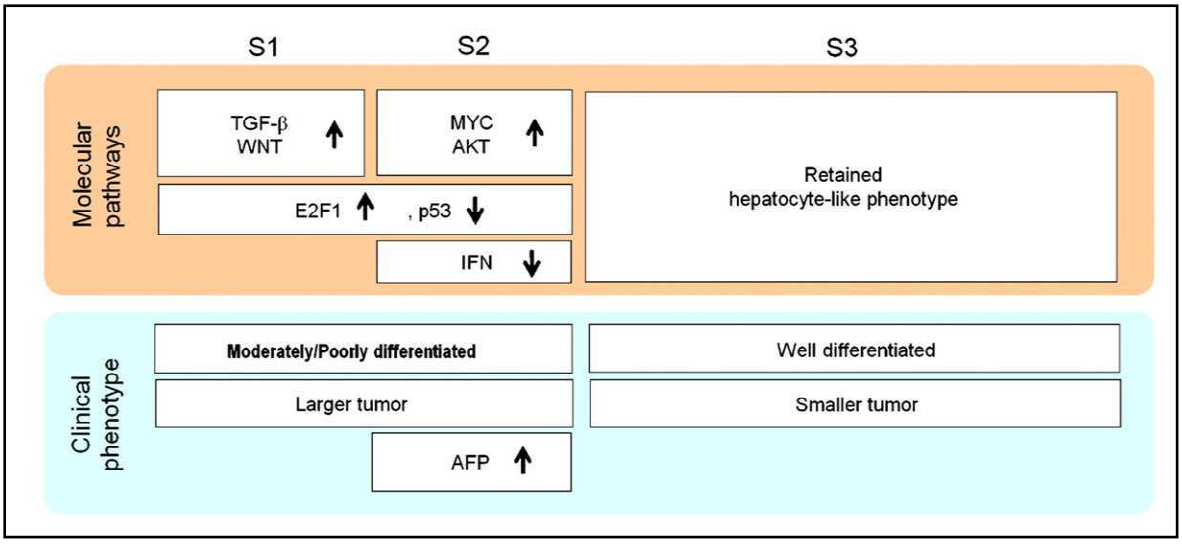

Figure 3. Molecular classification of HCC (Hoshida *et al.*, 2009). Subclasses S1, S2 and S3 show distinct molecular characteristics.

Clinical classification of HCC

In the management of HCC, a classification system is an important component to determine subgroups of patients and to supply them with reasonable treatment (Llovet *et al.*, 2003). Various classification systems are available for HCC, of which one of the most popular ones is the Tumor-Node-Metastasis (TNM) classification. According to the International Union against cancer (UICC), the TNM staging is based on the size of tumor (T), the status of lymph nodes near the tumor (N) and the presence of metastasis (M) (Thiery, 2002). However, it was found that this system may not be very helpful for prognosis because it does not evaluate the underlying liver disease, which is a major cause of mortality in patients with HCC (Schafer and Sorrell, 1999).

In the last years the Barcelona Clinic Liver cancer classification (BCLC) has emerged as a standard classification (Llovet *et al.*, 2003). It was presented for the first time in the journal 'Seminars in Liver disease' in 1999 (Llovet *et al.*, 1999). The main prognostic factors of this staging system are related to the tumor status (number and size of nodules, vascular invasion, extrahepatic spread), the liver function (defined by the Child Pugh score system, serum

bilirubin, serum albumin, portal hypertension) and general health status (defined by the Eastern Cooperative Oncology group [ECOG]) (Llovet *et al.*, 2008a). The current BCLC categories and the corresponding therapeutic strategies are shown in Figure 4.

A very early stage (stage 0) is defined as a single HCC nodule with a diameter of ≤ 2cm employing a normal liver function and diagnosed as carcinoma in situ. These patients are optimal candidates for resection and show a 5 year survival rate of 90% after treatment (Forner *et al.*, 2010).

Early stage HCC (stage A) classification is determined by one to three nodules with a diameter of < 3 cm. The liver function is defined by Child Pugh A or Child Pugh B status. Dependent on their liver function and tumor size, patients should be considered for radical therapy like resection, liver transplantation or local ablation via percutaneous ethanol injection (PEI) or radiofrequency ablation (RF) (Forner *et al.*, 2010; Greten *et al.*, 2005; Llovet and Bruix, 2003).

Intermediate stage HCC (stage B) is characterized by a preserved liver function with a large or multifocal tumor, no vascular invasion or extrahepatic spread and the absence of symptoms. Untreated patients suffering from intermediate stage HCC have a median survival of approximately 16 months (Llovet and Bruix, 2003). These patients can benefit from transarterial chemoembolisation (TACE) (Bruix and Llovet, 2009), which results in a median outcome of 20 months (Forner *et al.*, 2010).

In advanced stage HCC (stage C), vascular invasion or extrahepatic spread is detected and the patients suffer already from disease-related symptoms. The median survival is about 7 months and the outcome is mostly depending on the liver function. It was found that the multitarget tyrosine kinase inhibitor sorafenib improves survival of advanced stage HCC patients. The median overall survival was 10.7 months for sorafenib vs 7.9 months for placebo (Zhang *et al.*, 2010).

End stage (stage D) HCC includes those patients with a high tumor burden associated with an ECOG performance status of 3 or 4. These patients have a median survival of 3 months and only palliative therapies are possible (Llovet *et al.*, 2003).

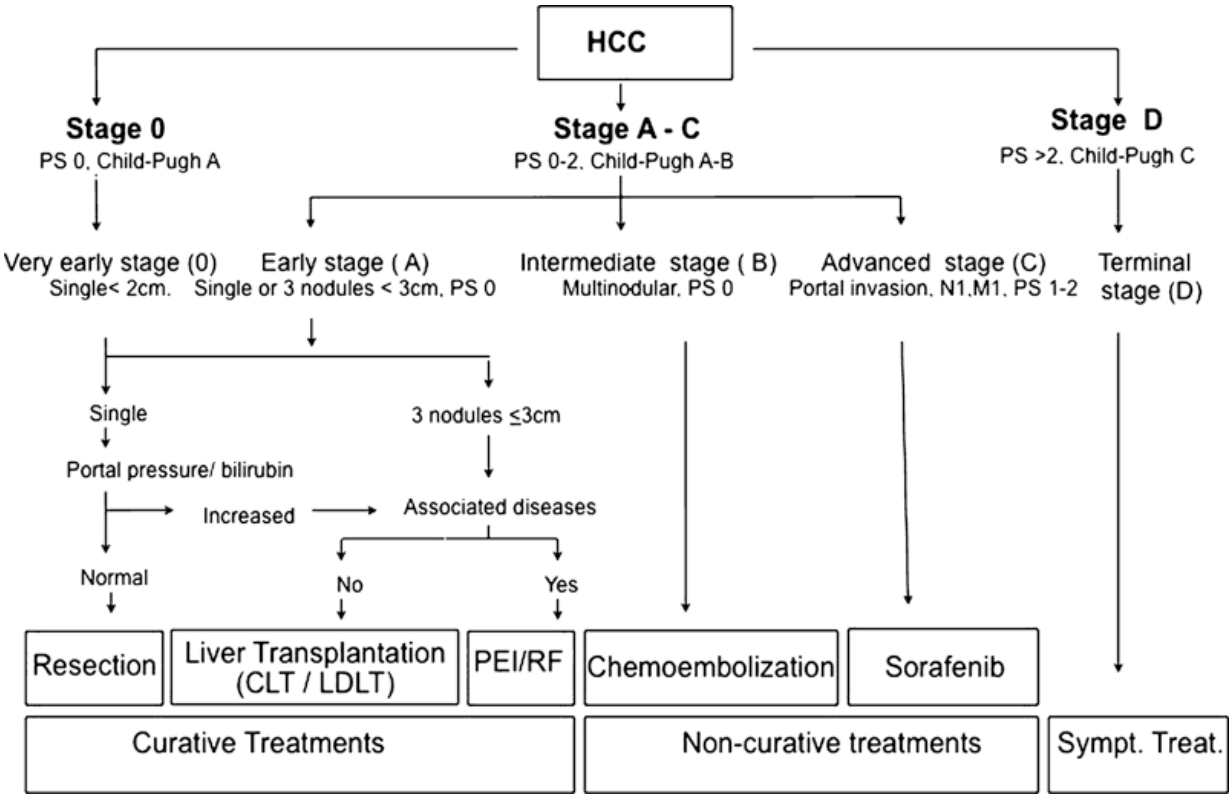

Figure 4. Barcelona Clinic liver cancer staging and treatment recommendation (Forner *et al.*, 2010). HCC patients can be grouped into five stages depending on tumor burden, liver function and physical status: very early (0), early (A), intermediate (B), advanced (C) and end (D) stage HCC. Staging is further connected to the recommended treatment option. CLT, cadaveric liver transplantation; LDLT, living donor liver transplantation; PEI, percutaneus ethanol injection; RF, radiofrequency ablation.

2.3. Treatment of HCC

Only 30-40% of all HCC patients are eligible for curative treatments (Llovet *et al.*, 2003). In those patients, resection and liver transplantation result in 5-year survival rates of 70% and local ablation therapies reach about 50% (Llovet *et al.*, 2003). Because many patients are not eligible for resection, therapy of unresectable HCC has been under extensive research in the past decades (Llovet and Bruix, 2003). HCC develops mostly in the setting of cirrhosis involving impaired liver function. The liver is the main organ for metabolism and cirrhosis decreases the activity of drug metabolizing enzymes and alters the absorption, plasma protein binding, distribution, and renal excretion of drugs (Thomas and Abbruzzese, 2005).

For unresectable HCC, treatment options depend mostly on the stage of the disease. 50% of HCC patients are diagnosed at an intermediate to advanced stage (Greten *et al.*, 2005) due to the lack of symptoms during early stages and the rapid progression of the disease (Sun and Sarna, 2008). Patients with intermediate stage HCC can benefit from transarterial embolisation (TAE)/TACE.

The blood supply of healthy liver is covered by 85% from the portal vein and only 5% from the hepatic artery. In contrast, in HCC the blood mainly originates from the hepatic artery, thus TAE/TACE is one therapy of choice. TAE induces the obstruction of the hepatic artery using embolising agents such as an absorbable gelatine sponge, or alcohol, to induce tumor necrosis. During TACE, chemotherapeutic agents get injected into the artery and subsequently arterial obstruction is performed. With this method it is possible to use high drug doses which is constricted specifically to the tumor area and thus, systemic toxicity can be minimized (Rampone *et al.*, 2009). A meta – analysis of several studies showed, that chemoembolization with doxorubicin or cisplatin improves survival of patients with unresectable HCC (Llovet and Bruix, 2003). One of the recent achievement was the development of drug eluting beads

(DEB) which induce arterial obstruction and release simultaneously a chemotherapeutic drug such as doxorubicin (Forner and Trinchet, 2009; Varela *et al.*, 2007).

In advanced stages of HCC, curative therapies are no longer possible. Because of the advanced stage of cirrhosis and reduced liver function also systemic treatment is a major challenge and thus was under extensive research (Schwartz *et al.*, 2007). The finding that estrogens may promote liver tumor growth (Francavilla *et al.*, 1989) has led many investigators to test hormonal therapy. Tamoxifen, an antiestrogenic compound, was tested in several studies but it failed to improve survival in patients with advanced HCC (Zhu, 2006). Other hormonal therapies like anti-androgens or octreotide, a somatostatine analogue, showed also no benefit (Lopez *et al.*, 2006). Systemic treatment with doxorubicin, the most widely used agent in HCC, was tested but the outcomes remain almost inconclusive (Zhu, 2006). Chemotherapeutics such as epirubicin, cisplatin, 5-fluoruracil or the combination of cisplatin, interferon alpha, doxorubicin and 5-fluoruracil (PIAF) have failed to demonstrate a significant acitivtiy (Zhu, 2006). Other compounds like noatrexed, a thymidilate synthase inhibitor, seocalocitol, a vitamin D-like antiproliferative molecule, or a tubulin inhibitor (T-67) also showed no benefits in treatment of HCC in randomized controlled trials (RCTs) (Llovet and Bruix, 2008).

With the improvement in understanding the molecular mechanisms of hepatocarcinogenesis, new molecular targeted agents have been developed. Recently it was shown that sorafenib, which targets Raf-1, B-Raf, VEGFR1&2 and PDGFR improves survival of patients with advanced HCC (Cheng *et al.*, 2009; Llovet *et al.*, 2008b; Wilhelm *et al.*, 2006). This was a major breakthrough in treatment of advanced HCC and gives the rationale to develop further molecular targeted therapies against this otherwise rather chemoresistant tumor. Several molecular therapies have been tested in pre-clinical studies and clinical trials. They can be summarized in 4 different groups of targets (Figure 5; Llovet and Bruix, 2008).

1. Inhibitors of EGFR: erlotinib, gefitinib, lapatinib, cetuximab. Only erlotinib showed an activity in pre-clinical and clinical studies, whereas the efficacies of the other compounds showed inconclusive results and thus remain to be further elucidated (Llovet and Bruix, 2008).
2. Inhibitors of angiogenic factors: humanized monoclonal antibodies such as bevacizumab and small molecules such as sorafenib, sunitinib, brivanib. HCC are mostly highly vascularized tumors and it was shown that VEGF, PDGF and angiopoeitin are often upreguated in this disease (Farazi and DePinho, 2006). Bevacizumab, an antibody against VEGF in combination with erlotinib was shown to have an antitumoral activity (Thomas *et al.*, 2009). Sunitinib was compared in a phase III randomized study to sorafenib, but although they have similar targets, sunitinib shows more toxic effects (Zhu *et al.*, 2009) and the study had to be terminated (Clinicaltrials.gov NCT00699374). The data from some first line treatments of HCC with brivanib seem to be promising and a phase III study is ongoing (NCT00858871) (Finn, 2010)
3. Inhibitors of PI3K/Akt/mTOR: everolimus and temsirolimus. About 50% of HCC patients have an activation of the mTOR pathway (Villanueva *et al.*, 2008). Preclinical in vitro data showed that mTOR inhibition by rapamycin and analogues reduces HCC growth and improves survival (Sahin *et al.*, 2004). Phase II studies are currently testing analoges of rapamycin including everolimus and temsirolimus alone or in combination with sorafenib (Llovet and Bruix, 2008).
4. Inhibitors of c-met, IGFR1 and Wnt. The Wnt pathway is activated in 33% to 67% of HCCs (Lee *et al.*, 2006a). At the moment there are no drugs available that can block its activation without causing significant side effects. Other studies with inhibitors against IGFR1 or c-Met are ongoing (Llovet and Bruix, 2008).

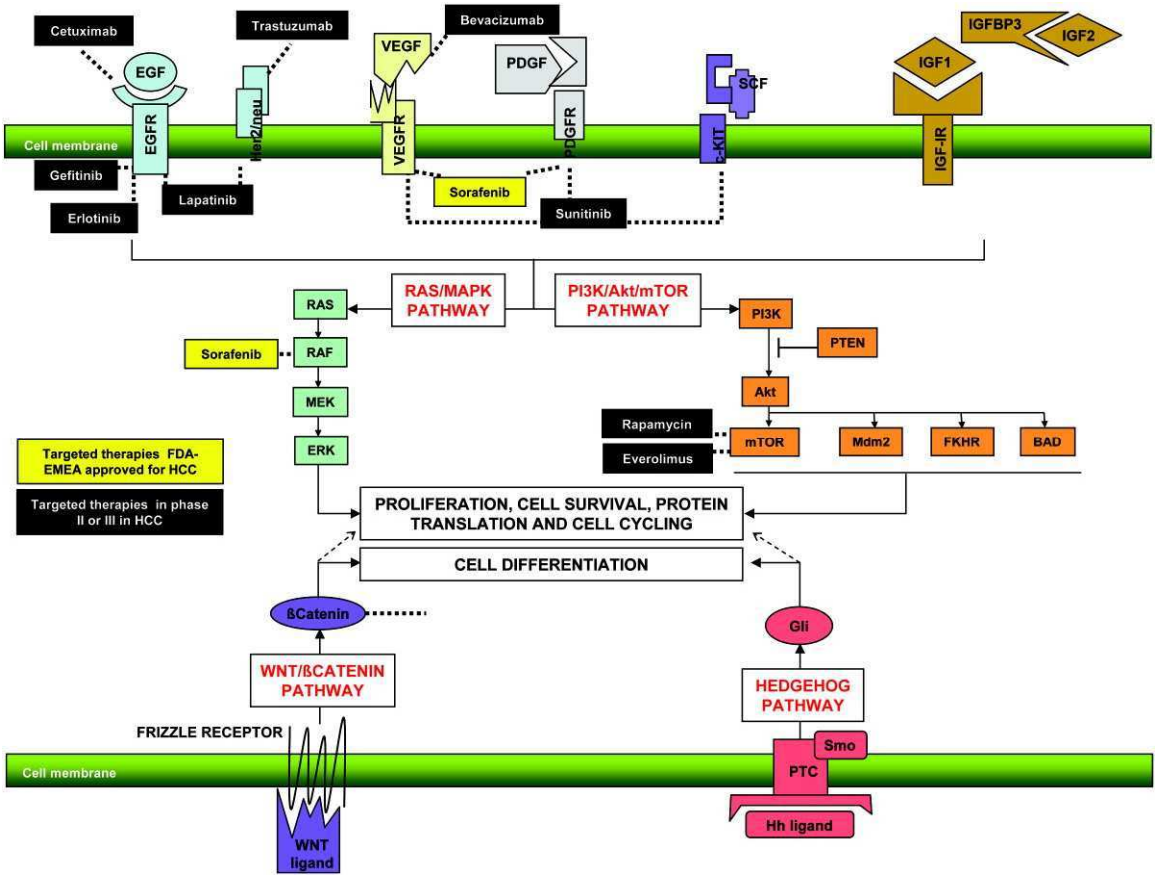

Figure 5. Key pathways in hepatocarcinogenesis and molecular targeted therapies currently used in preclinical or clinical trials (Llovet and Bruix, 2008). Monoclonal antibodies against VEGF (Bevacizumab) and EGFR (cetuximab), tyrosine kinase inhibitors against VEGFR (sorafenib, sunitinib), PDGFR (sorafenib, sunitinib), EGFR (erlotinib, lapatinib, AEE788) and Her2/neu (lapatinib, AEE788); tyrosine kinase inhibitors against Raf (sorafenib) mTOR (rapamycin, everolimus) and PI3K (XL-765)

2.4. Epithelial to mesenchymal transition - EMT

Epithelial to mesenchymal transition is described as a process where epithelial cells lose their polarization and cell-cell contacts by concomitant acquisition of a mesenchymal gene expression associated with increased motility (Figure 6). Epithelial cells are organized in layers and form basolateral adherens junctions composed of E-cadherin, catenins and actin-rings along with desmosomes as well as tight junctions, which represent apical polarity complexes. Integrins anchor the cells to the extracellular matrix via hemidesmosoms and focal adhesions. During EMT cells loose both, adherence and tight junctions, leading to the loss of the cell polarity and gain of mesenchymal and migratory traits. Cytoskeletal rearrangement by actin stress fibre formation and expression of matrix metalloproteinases favors cellular migration and invasion (Acloque *et al.*, 2009).

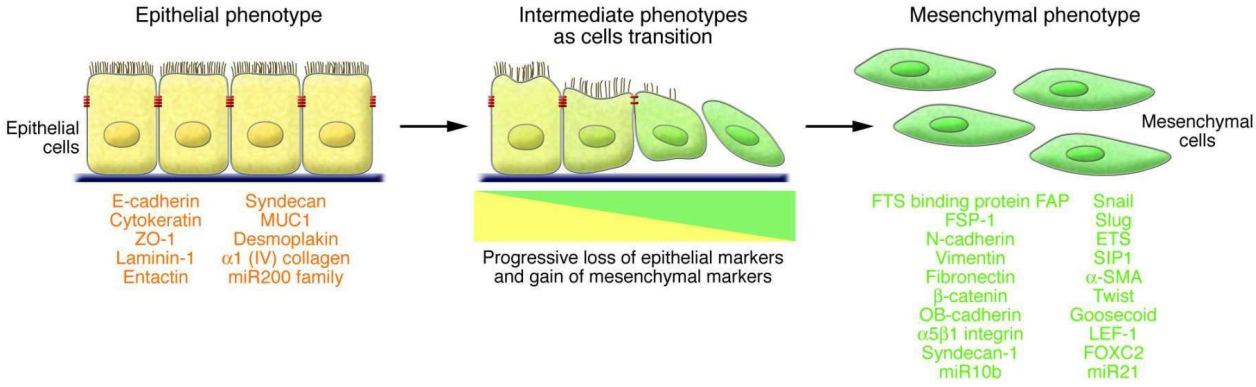

Figure 6. Process of EMT (Kalluri, 2009). EMT is a functional transition of polarized epithelial cells with adherence and tight junctions into mobile mesenchymal cells. Common EMT markers for epithelial and mesenchymal cells are listed. ZO-1, zonula occludens 1; MUC1, Mucin 1; cell surface associated, miR200, microRNA 200; FSP-1, fibroblast specific protein 1; SIP1, survival of motor neuron protein interacting protein 1; FOXC2, forkhead box C2.

On physiological conditions, EMT is crucial for an appropriate embryonic development. Epithelial cells show a high plasticity and can switch from an epithelial to an mesenchymal status and vice versa using the opposite process named mesenchymal to epithelial transition (MET; Thiery, 2002). In adults EMT occurs during wound healing, tissue regeneration and organ fibrosis to generate repair-associated mesenchymal cells. Furthermore, EMT is also involved in cancer progression, where it enables epithelial cancer cells to move locally and systemically into tumor surrounding tissues (Kalluri, 2009). Beside invasive and metastatic events in cancer progression, EMT participates also in other events that may be involved in tumor progression, including resistance to cell death and senescence, resistance to chemotherapy and immunotherapy as well as immune surveillance, immune suppression and inflammation (Thiery *et al.*, 2009).

All in all, EMT can be grouped in 3 different subtypes (Figure 7; Kalluri and Weinberg, 2009). Type 1 EMT is involved in implantation, embryo formation, organ development and generates mesenchymal cells to create new tissues with specific functions. Fibrosis or uncontrolled cell-invasion are absent in this type. Type 2 EMT is associated with wound healing, tissue regeneration and organ fibrosis. In this context EMT is a part of a repair mechanism in which fibroblasts are generated to reconstitute and repair tissues after injury or inflammation. When an inflammation remains chronically, however, type 2 EMT can lead to organ fibrosis and finally to destruction of the organ (Kalluri and Weinberg, 2009). The third proposed subtype is EMT type 3, which was shown to be associated with cancer progression and metastasis. This type occurs in epithelial cells that show already genetic or epigenetic changes, i.e. mutations in oncogenes or tumor suppressor genes. During type 3 EMT, cancer cells acquire migratory, invasive and metastatic properties (Kalluri and Weinberg, 2009).

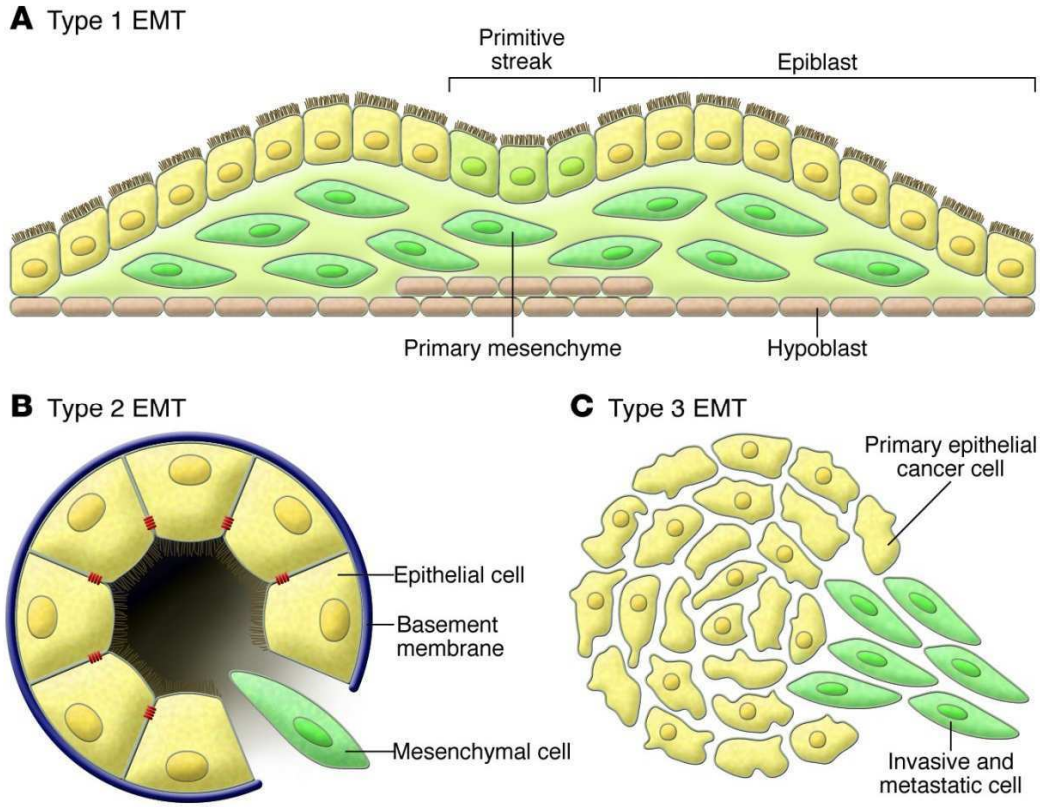

Figure 7. Different subtypes of EMT (Kalluri and Weinberg, 2009). (A) Type 1 EMT is associated with gastrulation in embryonic development. The primitive epithelium develops via EMT to the primary mesenchyme, which subsequently can form the secondary epithelia by MET. (B) Type 2 EMT give rise to fibroblasts which are involved in repair mechanisms of inflammation and fibrosis, whereas (C) type 3 EMT is involved in cancer progression and enable cells to invade and metastasize.

Molecular mechanisms of EMT

The expression of E-cadherin in adherence junctions is essential for the maintenance of the epithelial phenotype in tissues. Downregulation of E-cadherin has been shown to play a crucial role in EMT during development and tumorigenesis. It leads to a loss of cell-cell contacts, followed by the loss of cell polarity and further the translocation of β-catenin into the nucleus where it acts as a transcriptional activator of different oncogenes (Thiery, 2002). Different transcription factors were identified to be direct or indirect repressors of E-cadherin transcription, including Snail (Batlle *et al.*, 2000), the basic helix-loop-helix (bHLH) transcription factors E47 and Twist, the Zinc finger E-box binding homeobox (ZEB) factors deltaEF1/ZEB1 as well as mothers against Decapentaplegic (Smad) interacting protein

(Sip)1/Zeb2 (Peinado *et al.*, 2007). Once expressed and activated, each of the transcription factors activate different intracellular singaling cascades involving ERK, MAPK, PI3K, Akt, Smads, RhoB, β-catenin lymphoid enhancer binding factor (LEF), Ras, c-Fos as well as β4integrins and α5integrin (Tse and Kalluri, 2007). In case of many carcinomas, EMT-inducing transcription factors can be activated by signals from the tumor associated stroma, particularly by HGF, EGF, PDGF and TGF-β (Kalluri and Weinberg, 2009; Thiery, 2002). Especially important among these regulators is TGF-β, which has an ambivalent role. On the one hand, TGF-β is an important suppressor of cell proliferation and helps to maintain tissue homeostasis. On the other hand, it can act also as a positive modulator of tumor progression and metastasis (Bierie and Moses, 2006). In this context, TGF-β can induce EMT through multiple mechanisms, including Smad signaling leading to differential expression of transcription factors and kinases and induce an autocrine TGF-β loop. Serveral studies showed that β-Catenin and LEF as well as PDGF cooperate with Smads, suggesting an important role of a TGF-β/Smad/LEF/PDGF axis in induction of EMT (Kalluri and Weinberg, 2009). Another mechanism is the phosphorylation of partitioning defective protein 6 (PAR6A), which leads to the loss of cell polarity and loss of thight junctions (Ozdamar *et al.*, 2005). Recently, it was shown that TGF-β is a potent inducer of Snail expression, which is known to mediate resistance to apoptosis (Barrallo-Gimeno and Nieto, 2005). Beside autocrine factors, other pathways including the Wnt/β-catenin-, Notch- and Hedegog signaling have a major impact on EMT during development and cancer progression (Huber *et al.*, 2005).

Beside loosing epithelial traits, many studies showed that carcinoma cells express mesenchymal markers such as alpha smooth muscle actin (α-SMA), fibroblast specific protein (FSP)1, vimentin and desmin during the EMT process (Yang and Weinberg, 2008). These cells are mostly located at the invasive front of primary tumors and are prone to invade and metastasise. The invasion-metastasis cascade consists of multiple essential steps, including

invasion into the surrounding tissue, breaking through the basal membrane, intravasation into the lymph or the blood vessels, systemic dissemination and finally extravasation and colonization at a distant site of a competent organ via the MET-process (Figure 7; Fidler and Poste, 2008; Thiery, 2002).

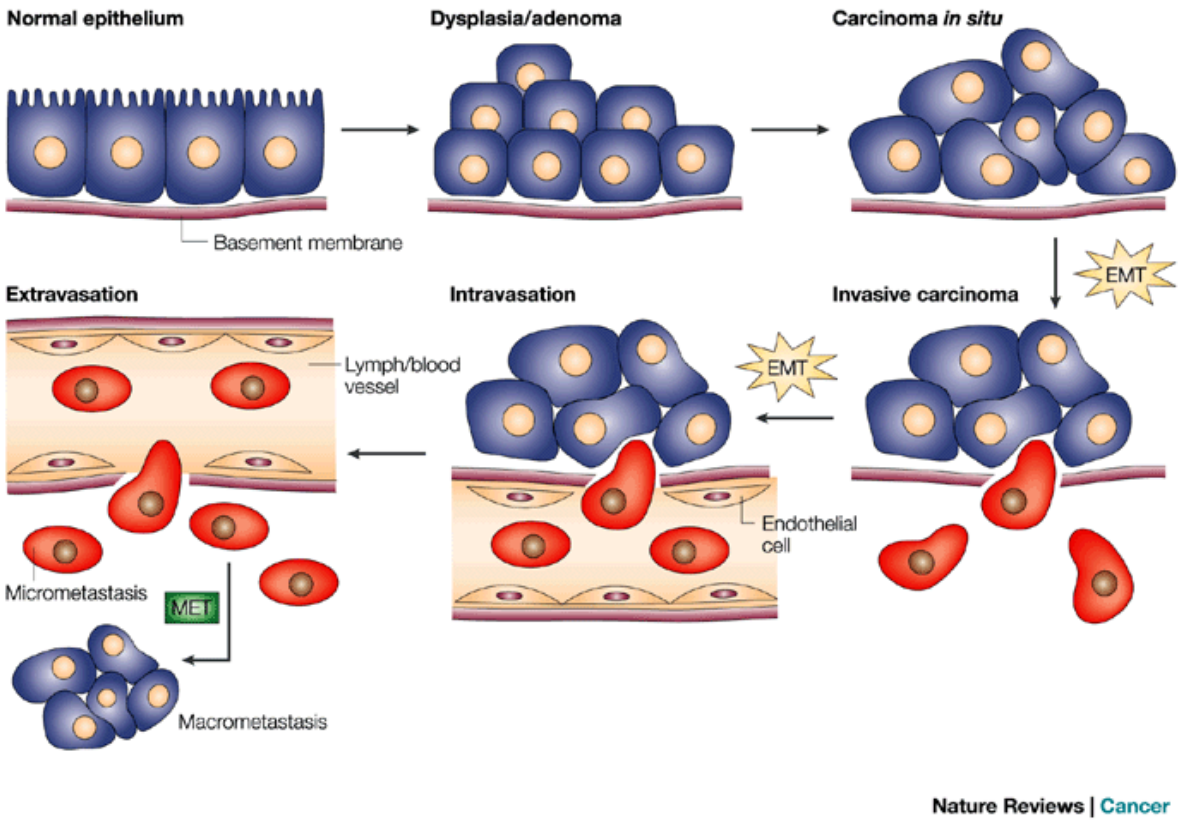

Figure 7. Steps in tumor progression (Thiery, 2002). After tumor initiation, a normal epithelium develops into an adenoma. Tumor promotion including genetic and epigenetic changes can further lead to the EMT process which is necessary for breaking through the basal membrane and subsequent intravasation and systemic spread. Extravasation and the MET process are essential for the development of distant metastases.

2.5. EMT in HCC

Several studies showed the occurrence of EMT during HCC development. Disruption of membrane-bound E-cadherin and β-catenin, the most important markers of EMT, were shown in 60,2% and 51,1% of primary HCC samples, respectively. The major regulators of EMT, Snail, Twist or Slug were identified in 43% to 56% of primary HCCs. HCC cell lines with increased Snail or Twist expression showed a higher invasive potential compared to cells with low Twist/Snail expression (Yang *et al.*, 2009). In line with that, Twist expression was found to correlate with HCC metastasis (Lee *et al.*, 2006b). In murine hepatocytes TGF-β was shown to induce EMT via disorganization of the epithelial cell membrane, downregulation of cytoskeletal proteins and upregulation of mesenchymal and invasive markers (Cicchini *et al.*, 2008). It was shown that Ha-Ras transformed murine hepatocytes convert from an epithelial to a fibroblastoid phenotype upon TGF-β1 treatment and regulate their TGFβ signaling in an autocrine fashion (Gotzmann *et al.*, 2002). These cells exhibited an accumulation of nuclear β-Catenin upon TGF-β treatment which has been even correlated with tumor recurrence in human HCC (Zulehner *et al.*, 2009).

In the past decades many novel factors which seem to play an important role in HCC progression were identified. In human HCC, blocking of TGF-βRI leads to increased expression of E-cadherin in the tumor and inhibits the synthesis of connective tissue growth factor (CTGF), produced by invasive tumor cells. This leads to diminished tumor growth, intravasation and metastatic dissemination of HCC cells (Mazzocca *et al.*, 2010; Mazzocca *et al.*, 2009). Furthermore, it was shown that TGF-β1 induces in cooperation with Laminin-5 (Ln-5) an EMT resulting in a higher invasiveness of HCC cells (Giannelli *et al.*, 2005). Another study showed that chromodomain helicase/ATPase DNA binding protein 1- like gene (CHD1L) induces EMT and increased cell motility through the Rho guanine nucleotide

exchange factor (ARHGEF)9 mediated activation of Cdc42 (Chen *et al.*, 2010). Furthermore, eukaryotic Initiation factor (EIF5A2) can induce EMT in HCC (Tang *et al.*, 2010).

Taken together, a multitude of studies showed the importance of EMT in HCC progression and the correlation with higher invasion and tumor recurrence. Thus, it is of a particular importance to investigate the molecular mechanisms underlying EMT in HCC progression in order to identify key regulators which can be used as novel targets for further development of promising anti cancer strategies.

2.6. Aim of the study

EMT is a crucial event in HCC progression and recurrence. Until now there is no available human cellular model for EMT in HCC. Yet, such a model will be highly useful to identify novel targets for therapy and to test novel anti-cancer agents. Thus, the primary aim of this study was to establish a cellular model of EMT which faithfully reflects HCC progression. With this model we aimed on the one hand to examine the efficacy and specificity of chemotherapeutics and targeted therapeutic drugs currently used in clinics either alone or in synergistic action. On the other hand, we aimed to identify new key regulators of EMT which may be potent targets for future therapy of HCC.

Data regarding the establishment of an unique human EMT model of HCC progression has been summarized in a manuscript which has already been submitted to a high-ranked scientific journal.

2.7. References

Acloque H, Adams MS, Fishwick K, Bronner-Fraser M, Nieto MA (2009). Epithelial-mesenchymal transitions: the importance of changing cell state in development and disease. *J Clin Invest* **119:** 1438-49.

Aravalli RN, Steer CJ, Cressman EN (2008). Molecular mechanisms of hepatocellular carcinoma. *Hepatology* **48:** 2047-63.

Barrallo-Gimeno A, Nieto MA (2005). The Snail genes as inducers of cell movement and survival: implications in development and cancer. *Development* **132:** 3151-61.

Batlle E, Sancho E, Franci C, Dominguez D, Monfar M, Baulida J *et al* (2000). The transcription factor snail is a repressor of E-cadherin gene expression in epithelial tumour cells. *Nat Cell Biol* **2:** 84-9.

Bierie B, Moses HL (2006). Tumour microenvironment: TGFbeta: the molecular Jekyll and Hyde of cancer. *Nat Rev Cancer* **6:** 506-20.

Blum HE, Spangenberg HC (2007). Hepatocellular carcinoma: an update. *Arch Iran Med* **10:** 361-71.

Bruix J, Llovet JM (2009). Major achievements in hepatocellular carcinoma. *Lancet* **373:** 614-6.

Calvisi DF, Ladu S, Gorden A, Farina M, Conner EA, Lee JS *et al* (2006). Ubiquitous activation of Ras and Jak/Stat pathways in human HCC. *Gastroenterology* **130:** 1117-28.

Cha C, Dematteo RP (2005). Molecular mechanisms in hepatocellular carcinoma development. *Best Pract Res Clin Gastroenterol* **19:** 25-37.

Chen L, Chan TH, Yuan YF, Hu L, Huang J, Ma S *et al* (2010). CHD1L promotes hepatocellular carcinoma progression and metastasis in mice and is associated with these processes in human patients. *J Clin Invest* **120:** 1178-91.

Cheng AL, Kang YK, Chen Z, Tsao CJ, Qin S, Kim JS *et al* (2009). Efficacy and safety of sorafenib in patients in the Asia-Pacific region with advanced hepatocellular carcinoma: a phase III randomised, double-blind, placebo-controlled trial. *Lancet Oncol* **10:** 25-34.

Chiang DY, Villanueva A, Hoshida Y, Peix J, Newell P, Minguez B *et al* (2008). Focal gains of VEGFA and molecular classification of hepatocellular carcinoma. *Cancer Res* **68:** 6779-88.

Cicchini C, Laudadio I, Citarella F, Corazzari M, Steindler C, Conigliaro A *et al* (2008). TGFbeta-induced EMT requires focal adhesion kinase (FAK) signaling. *Exp Cell Res* **314:** 143-52.

Coulouarn C, Factor VM, Andersen JB, Durkin ME, Thorgeirsson SS (2009). Loss of miR-122 expression in liver cancer correlates with suppression of the hepatic phenotype and gain of metastatic properties. *Oncogene* **28:** 3526-36.

Coulouarn C, Factor VM, Thorgeirsson SS (2008). Transforming growth factor-beta gene expression signature in mouse hepatocytes predicts clinical outcome in human cancer. *Hepatology* **47:** 2059-67.

Deli G, Jin CH, Mu R, Yang S, Liang Y, Chen D *et al* (2005). Immunohistochemical assessment of angiogenesis in hepatocellular carcinoma and surrounding cirrhotic liver tissues. *World J Gastroenterol* **11:** 960-3.

El-Serag HB, Mason AC (1999). Rising incidence of hepatocellular carcinoma in the United States. *N Engl J Med* **340:** 745-50.

El-Serag HB, Rudolph KL (2007). Hepatocellular carcinoma: epidemiology and molecular carcinogenesis. *Gastroenterology* **132:** 2557-76.

Farazi PA, DePinho RA (2006). Hepatocellular carcinoma pathogenesis: from genes to environment. *Nat Rev Cancer* **6:** 674-87.

Farazi PA, Glickman J, Jiang S, Yu A, Rudolph KL, DePinho RA (2003). Differential impact of telomere dysfunction on initiation and progression of hepatocellular carcinoma. *Cancer Res* **63:** 5021-7.

Fidler IJ, Poste G (2008). The "seed and soil" hypothesis revisited. *Lancet Oncol* **9:** 808.

Finn RS (2010). Development of molecularly targeted therapies in hepatocellular carcinoma: where do we go now? *Clin Cancer Res* **16:** 390-7.

Forner A, Reig ME, de Lope CR, Bruix J (2010). Current strategy for staging and treatment: the BCLC update and future prospects. *Semin Liver Dis* **30:** 61-74.

Forner A, Trinchet JC (2009). Transarterial therapies in HCC: does embolization increase survival? *J Hepatol* **51:** 981-3.

Francavilla A, Polimeno L, DiLeo A, Barone M, Ove P, Coetzee M *et al* (1989). The effect of estrogen and tamoxifen on hepatocyte proliferation in vivo and in vitro. *Hepatology* **9:** 614-20.

Giannelli G, Bergamini C, Fransvea E, Sgarra C, Antonaci S (2005). Laminin-5 with transforming growth factor-beta1 induces epithelial to mesenchymal transition in hepatocellular carcinoma. *Gastroenterology* **129:** 1375-83.

Gotzmann J, Huber H, Thallinger C, Wolschek M, Jansen B, Schulte-Hermann R *et al* (2002). Hepatocytes convert to a fibroblastoid phenotype through the cooperation of TGF-beta1 and Ha-Ras: steps towards invasiveness. *J Cell Sci* **115:** 1189-202.

Greten TF, Papendorf F, Bleck JS, Kirchhoff T, Wohlberedt T, Kubicka S *et al* (2005). Survival rate in patients with hepatocellular carcinoma: a retrospective analysis of 389 patients. *Br J Cancer* **92:** 1862-8.

Hanahan D, Weinberg RA (2000). The hallmarks of cancer. *Cell* **100:** 57-70.

Honda K, Sbisa E, Tullo A, Papeo PA, Saccone C, Poole S *et al* (1998). p53 mutation is a poor prognostic indicator for survival in patients with hepatocellular carcinoma undergoing surgical tumour ablation. *Br J Cancer* **77:** 776-82.

Hoshida Y, Nijman SM, Kobayashi M, Chan JA, Brunet JP, Chiang DY *et al* (2009). Integrative transcriptome analysis reveals common molecular subclasses of human hepatocellular carcinoma. *Cancer Res* **69:** 7385-92.

Huber MA, Kraut N, Beug H (2005). Molecular requirements for epithelial-mesenchymal transition during tumor progression. *Curr Opin Cell Biol* **17:** 548-58.

Imbeaud S, Ladeiro Y, Zucman-Rossi J (2010). Identification of novel oncogenes and tumor suppressors in hepatocellular carcinoma. *Semin Liver Dis* **30:** 75-86.

Ito Y, Takeda T, Sakon M, Tsujimoto M, Higashiyama S, Noda K *et al* (2001). Expression and clinical significance of erb-B receptor family in hepatocellular carcinoma. *Br J Cancer* **84:** 1377-83.

Ji J, Shi J, Budhu A, Yu Z, Forgues M, Roessler S *et al* (2009). MicroRNA expression, survival, and response to interferon in liver cancer. *N Engl J Med* **361:** 1437-47.

Kalluri R (2009). EMT: when epithelial cells decide to become mesenchymal-like cells. *J Clin Invest* **119:** 1417-9.

Kalluri R, Weinberg RA (2009). The basics of epithelial-mesenchymal transition. *J Clin Invest* **119:** 1420-8.

Kaseb AO, Hanbali A, Cotant M, Hassan MM, Wollner I, Philip PA (2009). Vascular endothelial growth factor in the management of hepatocellular carcinoma: a review of literature. *Cancer* **115:** 4895-906.

Kern SE, Pietenpol JA, Thiagalingam S, Seymour A, Kinzler KW, Vogelstein B (1992). Oncogenic forms of p53 inhibit p53-regulated gene expression. *Science* **256:** 827-30.

Laurent-Puig P, Legoix P, Bluteau O, Belghiti J, Franco D, Binot F *et al* (2001). Genetic alterations associated with hepatocellular carcinomas define distinct pathways of hepatocarcinogenesis. *Gastroenterology* **120:** 1763-73.

Lee HC, Kim M, Wands JR (2006a). Wnt/Frizzled signaling in hepatocellular carcinoma. *Front Biosci* **11:** 1901-15.

Lee TK, Poon RT, Yuen AP, Ling MT, Kwok WK, Wang XH *et al* (2006b). Twist overexpression correlates with hepatocellular carcinoma metastasis through induction of epithelial-mesenchymal transition. *Clin Cancer Res* **12:** 5369-76.

Llovet JM, Bru C, Bruix J (1999). Prognosis of hepatocellular carcinoma: the BCLC staging classification. *Semin Liver Dis* **19:** 329-38.

Llovet JM, Bruix J (2003). Systematic review of randomized trials for unresectable hepatocellular carcinoma: Chemoembolization improves survival. *Hepatology* **37:** 429-42.

Llovet JM, Bruix J (2008). Molecular targeted therapies in hepatocellular carcinoma. *Hepatology* **48:** 1312-27.

Llovet JM, Burroughs A, Bruix J (2003). Hepatocellular carcinoma. *Lancet* **362:** 1907-17.

Llovet JM, Di Bisceglie AM, Bruix J, Kramer BS, Lencioni R, Zhu AX *et al* (2008a). Design and endpoints of clinical trials in hepatocellular carcinoma. *J Natl Cancer Inst* **100:** 698-711.

Llovet JM, Ricci S, Mazzaferro V, Hilgard P, Gane E, Blanc JF *et al* (2008b). Sorafenib in advanced hepatocellular carcinoma. *N Engl J Med* **359:** 378-90.

Lopez PM, Villanueva A, Llovet JM (2006). Systematic review: evidence-based management of hepatocellular carcinoma--an updated analysis of randomized controlled trials. *Aliment Pharmacol Ther* **23:** 1535-47.

Massague J (2008). TGFbeta in Cancer. *Cell* **134:** 215-30.

Mazzocca A, Fransvea E, Dituri F, Lupo L, Antonaci S, Giannelli G (2010). Down-regulation of connective tissue growth factor by inhibition of transforming growth factor beta blocks the tumor-stroma cross-talk and tumor progression in hepatocellular carcinoma. *Hepatology* **51:** 523-34.

Mazzocca A, Fransvea E, Lavezzari G, Antonaci S, Giannelli G (2009). Inhibition of transforming growth factor beta receptor I kinase blocks hepatocellular carcinoma growth through neo-angiogenesis regulation. *Hepatology* **50:** 1140-51.

Meng F, Henson R, Wehbe-Janek H, Ghoshal K, Jacob ST, Patel T (2007). MicroRNA-21 regulates expression of the PTEN tumor suppressor gene in human hepatocellular cancer. *Gastroenterology* **133:** 647-58.

Minguez B, Tovar V, Chiang D, Villanueva A, Llovet JM (2009). Pathogenesis of hepatocellular carcinoma and molecular therapies. *Curr Opin Gastroenterol* **25:** 186-94.

Ozdamar B, Bose R, Barrios-Rodiles M, Wang HR, Zhang Y, Wrana JL (2005). Regulation of the polarity protein Par6 by TGFbeta receptors controls epithelial cell plasticity. *Science* **307:** 1603-9.

Parkin DM, Bray F, Ferlay J, Pisani P (2005). Global cancer statistics, 2002. *CA Cancer J Clin* **55:** 74-108.

Peinado H, Olmeda D, Cano A (2007). Snail, Zeb and bHLH factors in tumour progression: an alliance against the epithelial phenotype? *Nat Rev Cancer* **7:** 415-28.

Rampone B, Schiavone B, Martino A, Viviano C, Confuorto G (2009). Current management strategy of hepatocellular carcinoma. *World J Gastroenterol* **15:** 3210-6.

Sahin F, Kannangai R, Adegbola O, Wang J, Su G, Torbenson M (2004). mTOR and P70 S6 kinase expression in primary liver neoplasms. *Clin Cancer Res* **10:** 8421-5.

Schafer DF, Sorrell MF (1999). Hepatocellular carcinoma. *Lancet* **353:** 1253-7.

Schwartz M, Roayaie S, Konstadoulakis M (2007). Strategies for the management of hepatocellular carcinoma. *Nat Clin Pract Oncol* **4:** 424-32.

Sun VC, Sarna L (2008). Symptom management in hepatocellular carcinoma. *Clin J Oncol Nurs* **12:** 759-66.

Tang DJ, Dong SS, Ma NF, Xie D, Chen L, Fu L *et al* (2010). Overexpression of eukaryotic initiation factor 5A2 enhances cell motility and promotes tumor metastasis in hepatocellular carcinoma. *Hepatology* **51:** 1255-63.

Thiery JP (2002). Epithelial-mesenchymal transitions in tumour progression. *Nat Rev Cancer* **2:** 442-54.

Thiery JP, Acloque H, Huang RY, Nieto MA (2009). Epithelial-mesenchymal transitions in development and disease. *Cell* **139:** 871-90.

Thomas MB, Abbruzzese JL (2005). Opportunities for targeted therapies in hepatocellular carcinoma. *J Clin Oncol* **23:** 8093-108.

Thomas MB, Morris JS, Chadha R, Iwasaki M, Kaur H, Lin E *et al* (2009). Phase II trial of the combination of bevacizumab and erlotinib in patients who have advanced hepatocellular carcinoma. *J Clin Oncol* **27:** 843-50.

Thorgeirsson SS, Grisham JW (2002). Molecular pathogenesis of human hepatocellular carcinoma. *Nat Genet* **31:** 339-46.

Tse JC, Kalluri R (2007). Mechanisms of metastasis: epithelial-to-mesenchymal transition and contribution of tumor microenvironment. *J Cell Biochem* **101:** 816-29.

Varela M, Real MI, Burrel M, Forner A, Sala M, Brunet M *et al* (2007). Chemoembolization of hepatocellular carcinoma with drug eluting beads: efficacy and doxorubicin pharmacokinetics. *J Hepatol* **46:** 474-81.

Villanueva A, Chiang DY, Newell P, Peix J, Thung S, Alsinet C *et al* (2008). Pivotal role of mTOR signaling in hepatocellular carcinoma. *Gastroenterology* **135:** 1972-83, 1983 e1-11.

Wilhelm S, Carter C, Lynch M, Lowinger T, Dumas J, Smith RA *et al* (2006). Discovery and development of sorafenib: a multikinase inhibitor for treating cancer. *Nat Rev Drug Discov* **5:** 835-44.

Yang J, Weinberg RA (2008). Epithelial-mesenchymal transition: at the crossroads of development and tumor metastasis. *Dev Cell* **14:** 818-29.

Yang MH, Chen CL, Chau GY, Chiou SH, Su CW, Chou TY *et al* (2009). Comprehensive analysis of the independent effect of twist and snail in promoting metastasis of hepatocellular carcinoma. *Hepatology* **50:** 1464-74.

Yao DF, Wu XH, Zhu Y, Shi GS, Dong ZZ, Yao DB *et al* (2005). Quantitative analysis of vascular endothelial growth factor, microvascular density and their clinicopathologic features in human hepatocellular carcinoma. *Hepatobiliary Pancreat Dis Int* **4:** 220-6.

Zhang T, Ding X, Wei D, Cheng P, Su X, Liu H *et al* (2010). Sorafenib improves the survival of patients with advanced hepatocellular carcinoma: a meta-analysis of randomized trials. *Anticancer Drugs* **21:** 326-32.

Zhu AX (2006). Systemic therapy of advanced hepatocellular carcinoma: how hopeful should we be? *Oncologist* **11:** 790-800.

Zhu AX, Sahani DV, Duda DG, di Tomaso E, Ancukiewicz M, Catalano OA *et al* (2009). Efficacy, safety, and potential biomarkers of sunitinib monotherapy in advanced hepatocellular carcinoma: a phase II study. *J Clin Oncol* **27:** 3027-35.

Zulehner G, Mikula M, Schneller D, van Zijl F, Huber H, Sieghart W *et al* (2009). Nuclear beta-catenin induces an early liver progenitor phenotype in hepatocellular carcinoma and promotes tumor recurrence. *Am J Pathol* **176:** 472-81.

3. Manuscript

A unique human model to monitor drug efficacy in hepatocellular carcinoma progression

Franziska van Zijl[1†], Sabine Mall[1†], Georg Machat[1], Christine Pirker[1], Robert Zeillinger[2], Andreas Weinhäusel[3], Martin Bilban[4], Walter Berger[1], Wolfgang Mikulits[1*]

[1]Department of Medicine I, Division: Institute of Cancer Research, Medical University of Vienna, Borschkegasse 8a, 1090 Vienna; [2]Ludwig Boltzmann Institute for Gynecology and Gynecological Oncology, Department of Obstetrics and Gynecology, University of Vienna, Waehringer Guertel 18-20, 1090 Vienna; [3]Austrian Institute of Technology, Seibersdorf; [4]Clinical Institute for Medical and Chemical Laboratory Diagnostics, Medical University of Vienna, Währingerstraße 18-20, 1090 Vienna, Austria.

***Corresponding author.** Tel.: +43 1 4277 65250; fax: +43 1 4277 65239; E-mail address: wolfgang.mikulits@meduniwien.ac.at (W. Mikulits)

[†]These authors contributed equally to this work.

Abbreviations: CGH, comparative genomic hybridization; EMT, epithelial to mesenchymal transition; HCC, hepatocellular carcinoma; IC, inhibitory concentration; TACE, transarterial chemoemolisation; TGF, transforming growth factor.

Financial disclosure: There are no financial disclosures relevant to this manuscript.

3.1. Abstract

Background & Aims: The epithelial to mesenchymal transition (EMT) of malignant hepatocytes is a crucial event in hepatocellular carcinoma (HCC) progression and recurrence. We aimed to establish an EMT model of human HCC to examine drug efficacy and specificity in HCC progression.

Methods: Two liver cell lines were established from one HCC patient showing either an epithelial or mesenchymal phenotype. HCC cell populations were characterized by immunofluorescence analysis, migration and invasion assays, comparative genomic hybridization (CGH), whole-genome expression profiling and promoter methylation. Therapeutic agents clinically used against HCC were examined for efficacy by determination of IC_{50} values.

Results: Isolated HCC cells displayed an epithelial and a mesenchymal phenotype of which latter showed strong migratory and invasive abilities *in vitro*. CGH analysis indicated a common cellular origin of both cell types, suggesting that mesenchymal HCC cells have been derived from epithelial hepatocytes through EMT *in vivo*. Whole-genome expression profiling showed loss of epithelial as well as gain of mesenchymal markers, verifying EMT. Drug exposure of mesenchymal HCC cells showed higher resistance to the targeted therapeutic agents sorafenib and erlotinib as compared to epithelial HCC cells, which were slightly more resistant to cytostatic drugs. Most remarkably, combined treatment of doxorubicin and sorafenib caused increased susceptibility of both HCC cell types resulting in enhanced drug efficacy by lowered IC_{50} values.

Conclusion: The unique EMT model of human HCC allows the identification of molecular mechanisms and pre-clinical studies to assess therapeutic drug effectiveness during liver cancer progression.

Key words: hepatocellular carcinoma; epithelial to mesenchymal transition; drug efficacy.

3.2. Introduction

The epithelial to mesenchymal transition (EMT) enables carcinoma cells to invade into surrounding tissues and to form secondary tumors known as metastases. A particular characteristic of EMT is the downregulation of E-cadherin expression, which causes disruption of cell-cell junctions and dissemination of cells from the primary tumor [1]. Dysregulation of E-cadherin is provoked by its transcriptional repressors involving Snail/SNAI1, Slug/SNAI2, ZEB1/ΔEF1, ZEB2/SIP1 or Twist [2]. Receptor tyrosine kinase (RTK)/Ras and transforming growth factor (TGF)-β signaling as well as Wnt/β-catenin-, Notch-, Hedgehog- and NF-κB-dependent pathways can induce and maintain EMT during cancer progression [1, 3].

The pivotal role of EMT in hepatocellular carcinoma (HCC) has been increasingly recognized and various molecular mechanisms of hepatocellular EMT have been identified [4, 5]. In human HCC, EMT correlates with invasive tumors, intrahepatic metastasis and poor survival [6]. This is of particular relevance since intrahepatic metastases were observed in more than 30% of HCC cases after liver surgery and in 80% of HCC autopsy cases [7].

Epidemiologically, HCC has a poor prognosis and represent the third most cause of death from cancer worldwide due to diagnosis at advanced stages and lack of effective therapy options [8]. Thus, HCC therapy is hampered by the fact that the liver is central for xenobiotic metabolism resulting in rapid modifications and efflux of drugs. Curative therapies such as resection and liver transplantation are applicable in only 15% of HCC patients [9] and show a high incidence of recurrence [10]. Unresectable HCC are treated with locoregional therapies involving transarterial chemoembolization (TACE), percutaneous ethanol injection or radiofrequency ablation [11]. TACE represents an intra-arterial administration of therapeutic drugs combined with embolizing agents which leads to a more selective distribution and a higher retention time of therapeutics within HCC. TACE has been established as the standard

therapy for patients with intermediate stage cancer [12], although the efficacy of TACE is limited and patients often suffer from recurrence [13]. The most frequently used chemotherapeutics for TACE are doxorubicin, cisplatin and epirubicin, either alone or in combination [14], from which doxorubicin or cisplatin showed significant benefits [13]. Moreover, targeted therapeutic agents such as the multikinase inhibitor sorafenib has been shown to have survival benefits especially in patients with advanced stage HCC [15-17]. Those studies are the basis to develop treatment modalities to efficiently combat HCC progression that is considered as utmost treatment-resistant. However, suitable human HCC models are required to identify potential molecular targets, to test drug efficacy and to estimate the effective concentration of therapeutic agents.

Here, we established a human model of EMT which reflects important aspects of HCC progression and allows to study its underlying molecular mechanisms. The matched pair of epithelial and mesenchymal HCC cells enables us (i) to evaluate the efficacy of currently used therapeutic agents in single or combined treatments and (ii) to assess the effectiveness of novel anti-cancer agents during HCC progression.

3.3. Material and Methods

Cell culture

HCC-1.2 and HCC-1.1 cells, referred to as 3p and 3sp cells, respectively, were isolated from one HCC patient as described [18]. 3p cells of passages 10 to 12 and 3sp cells of passages 7 to 13 are termed 3p early and 3sp early, respectively. 3p cells between passage 71 and 76 and 3sp from passage 72 to 87 were termed 3p late and 3sp late, respectively. Without particular designation of 3p and 3sp cells, passage numbers between 40 and 50 were employed. Details are described in Supplementary Material and Methods.

Quantitative Real Time PCR

PCR reactions were performed with Fast SYBR Green Master Mix (Applied Biosystems, Foster city, CA, USA) in duplicates according to the recommendations of the manufacturer and quantified with the 7500 Fast Real Time PCR System (Applied Biosystems, CA, USA). Arbitrary units were calculated by the dCT method. Forward and reverse primers are described in Supplementary Table 1.

Confocal immunofluorescence microscopy

Cells were seeded onto SuperFrostPlus glass slides (Menzel, Vienna, Austria) and fixed with either 4% paraformaldehyde or methanol/aceton. Staining with antibodies and nuclei is described in Supplementary Material and Methods.

Proliferation analysis

1.5×10^4 cells were plated and cell numbers were determined after various time points with a multichannel cell analyzer (CASY; Schärfe Systems, Reutlingen, Germany). Three independent experiments were performed in triplicates.

Cell migration and invasion assays

Cell migration and cell invasion was determined by Platypus Technology according to the manufacturer's protocol (Oris™ Cell Invasion & Detection Assay, Madison, USA). To analyze cell migration, 5 x 10^4 cells were plated onto 8 not-coated wells. To examine cell invasion, same cell numbers were seeded into 8 basal membrane extract (BME; 3.5mg/ml)-coated wells and overlaid with undiluted BME. Migration and invasion of cells was microscopically analyzed and quantitatively evaluated by measuring the fluorescence after staining with CellTracker™ (Green CMFDA; Invitrogen, Carlsbad, USA).

Comparative genomic hybridization (CGH)

Genomic DNA was isolated from early and late 3p and 3sp HCC cells using the QIAamp DNA Blood Mini Kit (Qiagen, Hilden, Germany) according to manufacturer's protocol. CGH analysis was performed using human 4x44K whole genome oligonucleotide-based arrays (Agilent, Santa Clara, USA). Details are described in Supplementary Material and Methods.

Expression profiling using microarrays

Total RNA was isolated from duplicates of early and late 3p and 3sp HCC cells using the RNAeasy kit (Qiagen, Hilden, Germany). The integrity and quantity of RNA was analyzed by Agilent Bioanalyzer (Agilent Technologies, Santa Clara, USA). cRNA labeling and hybridization on Affymetrix GeneChip® Human gene 1.0 ST Array (Affymetrix, Santa Clara, USA) as well as scanning of signal intensities was performed according to the manufacturer's protocol. The ratio of regulation was calculated and a minimum of 3-fold regulation was considered as significant. Computational analysis was performed with Gene set enrichment analysis (GSEA) software (http://www.broad.mit.edu/gsea/msigdb/annotate.jsp) by comparing the molecular profile data with existing as well as self-defined gene sets.

Analysis of CpG methylation

Genomic DNA was isolated from 3p and 3sp HCC cells grown in quadruplicates and from primary peripheral blood cells using the QIAamp DNA Blood Mini Kit (Qiagen, Hilden, Germany). The digestion of 600 ng genomic DNA with methylation-sensitive restriction enzymes (MSRE) was performed. In total, 327 cancer-specific promoter loci were analyzed by PCR. Detailed procedure is described in Supplementary Material and Methods.

Therapeutic agents

Doxorubicin hydrochloride (adriamycin hydrochloride), cis-Diammineplatinum (II) dichloride (cisplatin) and epirubicin hydrochloride were purchased from Sigma, St Louis, USA and dissolved in 0,9% NaCl. Sorafenib (Nexavar®; Bayer HealthCare Pharmaceuticals, Wayne, USA), Erlotinib (Tarceva®; LC Laboratories, Woburn, USA) and Bevacizumab (Avastin®; Roche, Basel, Switzerland) were dissolved in dimethylsulfoxide (DMSO). Stock solutions were diluted in medium to concentrations indicated in the text.

Determination of the inhibitory concentration $(IC)_{50}$

Cell viability was determined using the 3-(4,5 dimethylthiazol-2-yl)-2,5-diphenyltetrazolium bromide (MTT) assay. Briefly, cells were seeded in triplicates at a density of 6×10^3 cells per well. After 24 hours, cells were incubated with drug-containing medium for three days. Cells were incubated with MTT solution (5mg/ml; Sigma, St Louis, USA) and after five hours medium was replaced with DMSO. The absorbance was measured at 620 nm by employing a microplate reader (Asys HiTech, Salzburg, Austria). MTT assays were repeated 3 times for each drug application and untreated cells were used as reference. IC_{50} values were obtained by log-linear interpolation of data points and are depicted by dose-response curves using the software GraphPad Prism® 5.01.

Statistical analysis

Data are expressed as means ± standard deviation (SD). The statistical significance of differences was evaluated using an unpaired, non-parametric Student’s t-test. Significant differences between experimental groups were * $p<0,05$, ** $p<0,01$ or *** $p<0,005$.

3.4. Results

HCC cells show an epithelial phenotype and a mesenchymal one correlating with enhanced cell motility.

Two distinct liver cell lines were isolated from the HCC of one patient [18]. Phase contrast analysis suggested an epithelial cell type, termed 3p, and a mesenchymal cell population, designated 3sp (Fig. 1A). Both HCC cells showed diploid DNA content (Supplementary Fig. 1) and short tandem repeat analysis verified their common genomic identity (Supplementary Table 2). qRT-PCR analysis revealed that 3p cells express epithelial markers such as E-cadherin and keratin 8, whereas 3sp cells showed a mesenchymal expression signature by upregulation of the transcription factors LEF1, SNAI1, SNAI2 and ZEB1 (Fig. 1B). Immunolocalization demonstrated intact adherence junctions by expression of E-cadherin, β-catenin and p^{120}catenin at cell borders of 3p cells, whereas 3sp cells failed to show this phenotype (Fig. 1C). In contrast to 3sp, 3p cells displayed cytoplasmic distribution of the epithelial marker keratin 8 by the concomitant absence of the mesenchymal interfilament component vimentin. In addition, mesenchymal 3sp cells showed relocalization of actin from the cell membrane to stress fibers suggesting enhanced motility.

We next assessed the migratory and invasive potential of 3p and 3sp cells. First, we performed proliferation kinetics to exclude an influence of differential cell doubling rates on migration and invasion assays. No significant difference in proliferation of 3p and 3sp cells could be detected (Fig. 2A). Yet, a 4-fold increased migratory potential of mesenchymal 3sp cells was determined when compared to 3p cells (Fig. 2B and 2C). To analyze invasion, HCC cells were embedded into matrigel. While epithelial 3p cells showed no invasive potential, mesenchymal 3sp cells displayed a more than 5-fold stronger ability to invade into the matrix (Fig. 2D and 2E). The invasive potential of mesenchymal 3sp cells was further analyzed by 3-dimensional (3D) spheroid formation in collagen gels [19]. Epithelial 3p cells formed

compact and round spheroids without cell invasion into the surrounding gel (Supplementary Fig. 2A), even though proliferation was not impaired (data not shown). On the contrary, mesenchymal 3sp cells failed to form spheroids on their own, however, these cells attached onto the surface of epithelial 3p-spheroids after co-cultivation, and showed strong invasion into the surrounding matrix (Supplementary Fig. 2A and 2B). Immunofluorescence analysis of E-cadherin and β-catenin indicated epithelial characteristics of 3p-derived spheroids, whereas these markers could not be detected in invading 3sp cells due to disassembly of epithelial junctions (Supplementary Fig. 2C). Taken together, 3p and 3sp cells showed a distinct epithelial and mesenchymal phenotype correlating with poor and strong migratory and invasive abilities, respectively.

Mesenchymal HCC cells developed through EMT in vivo.

We further investigated whether 3sp cells have been derived from 3p cells through EMT in the HCC patient. CGH analysis revealed a loss of genomic DNA in the TRPM3 and AXIN1 loci of both cell types (Fig. 3A and 3B). PCR analysis of multiple exons could identify the exact chromosomal breaks which are located between exon 12 and 15 and between exon 2 and 3 in TRPM3 and AXIN1, respectively (Supplementary Fig. 3). This homozygous loss of chromosomal regions indicates an identical cellular origin of 3p and 3sp hepatoma cells, and thus demonstrates that 3sp cells have been developed from 3p cells via EMT *in vivo*.

To verify EMT, we analyzed the 3p/3sp HCC cell lines by whole-genome expression profiling (Fig. 4A and 4B). Remarkably, a large cluster of liver-specific genes were downregulated in 3sp cells compared to 3p cells (Supplementary Fig. 4), including CYP450 phase I enzymes, alcoholdehydrogenase (ADH) and aldehydedehydrogenase (ALDH) and phase II enzymes such as UDP-glucuronosyl-transferases (UGT) and glutathione-S-tranferase (GST). Importantly, a cluster of epithelial markers involving components of tight junctions (claudins), desmosomes (desmoplakin) and adherence junctions (E-cadherin) were found to

be strongly downregulated in mesenchymal 3sp cells (Fig. 4A). Moreover, EMT-specific genes such as vimentin, LEF1 and SNAI2 were highly upregulated in 3sp cells (Fig. 4B), thus verifiying the expression analysis shown in Fig. 1B and 1C. In addition, expression profiling revealed (i) upregulation of growth factors and matrix metalloproteinases (MMPs) such as CTGF, TGF−β2 and MMP2, (ii) upregulation of receptors associated with EMT such as platelet-derived growth factor (PDGF)-Rβ and DDR2, and (iii) increase of EMT-associated proteins such as fibroblast activation protein, lysyl oxidase, tenascin C and SPARC (secreted protein, acidic and rich in cysteine). From these data we concluded that mesenchymal 3sp HCC cells were derived from epithelial 3p cells via EMT *in vivo*.

SPARC activation by CpG demethylation.

We next addressed the differences in the methylation status of gene promoters in 3p and 3sp cells. In order to exclude cell culture effects, genomic DNA of 3p/3sp cells from early as well as late passages was analyzed. Most notably, SPARC was identified to be epigenetically regulated, in line with a 128-fold upregulation of the transcript (Fig. 4B). Methylation-specific PCR of the SPARC promoter revealed a lowered methylation status in both early and late passaged mesenchymal 3sp cells (Fig. 4C), which was verified by qRT-PCR analysis showing a >30-fold increase of SPARC mRNA in 3sp cells (Fig. 4D). Since the CGH profile of the SPARC locus was unaffected, these data provide first evidence that the upregulation of SPARC is caused by demethylation during HCC progression.

The 3p/3sp EMT model is suitable for drug testing.

We next used this human HCC model to assess the efficacy of clinically used anti-cancer agents. Dose response relationships and corresponding half maximal inhibitory concentrations (IC_{50}) of drugs were determined (Table 1) and verified by viability assays (Supplementary Fig. 5A). Chemotherapeutics such as doxorubicin, cisplatin and epirubicin currently used for

TACE were compared to targeted therapeutic drugs such as the multikinase inhibitor sorafenib, the EGFR-inhibitor eroltinib and the VEGF inhibitor bevacizumab. 3sp cells showed a slightly higher susceptibility against chemotherapeutics when compared to 3p cells (Fig. 5A-C; Table 1), which is explained by downregulation of multiple drug resistance genes in 3sp cells (data not shown). Interestingly, 3sp cells were more resistant to targeted therapies including sorafenib and erlotinib (Fig. 5D and 5E; Table 1). Bevacizumab did not show an effect on neither of the cells (Fig. 5F, Table 1). The high sensitivity towards erlotinib is in line with the higher phosphorylation status of EGFR found in 3p cells (data not shown). Of particular interest was the higher resistance of 3sp cells towards sorafenib, as expression analysis showed a 10-fold upregulation of PDGFR-β (Fig. 4B). Additional targets of sorafenib including VEGFR-1, -2, -3 and RAF kinases were found unaltered between 3p and 3sp cells (data not shown). As PDGFR-β is described to play an important role in migration [20], we analyzed the migratory potential of 3sp cells upon sorafenib treatment (Supplementary Fig. 5B and 5C). Interestingly, delivery of sorafenib at the IC_{50} showed a strong reduction of migration, whereas control treatment of doxorubicin at the IC_{50} did not impair migration. Together, these data indicate that sorafenib has a lower cytotoxic potential on 3sp cells, however, strongly represses their migratory abilities.

In recent clinical efforts, sorafenib and doxorubicin were frequently used in combination therapy. Thus, we investigated the effect of the combined treatment of these anti-cancer drugs in our model of HCC progression. We therefore treated cells with one drug in increasing concentrations, while the second drug was kept constant at its IC_{50}. First, variable amounts of doxorubicin were applied in combination with the IC_{50} of sorafenib on 3p and 3sp cells (Fig. 6A). Compared to doxorubicin monotherapy, cells showed a drastic susceptibility for the combined treatment, leading to a reduction of the IC_{50} for doxorubicin of 60% and 39% in 3p and 3sp cells, respectively (Fig. 6B; Table 1). The vice versa treatment, applying variable amounts of sorafenib in combination with the IC_{50} of doxorubicin (Fig. 6C) showed a similar

result, leading to a reduction of the IC_{50} for sorafenib of 18% and 50% in 3p and 3sp cells, respectively (Fig. 6D; Table 1). Most interestingly, we observed a nomalization of the IC_{50} values between 3p and 3sp cells after combined treatment in both approaches (Fig. 6B and 6D, Table 1). Taken together, these results indicate that the monotherapy shows considerable differences in the susceptibility between HCC cells undergoing EMT. Our data provide evidence that the combined use of doxorubicin and sorafenib is highly efficient to target both epithelial and mesenchymal HCC cells.

3.5. Discussion

EMT has been increasingly recognized to play a crucial role in HCC progression by the acquisition of invasive properties. In line with the transdifferentiation of neoplastic hepatocytes to motile mesenchymal derivatives, HCC is described as a heterogenous tumor at advanced stages showing clonal expansion of genetically distinct malignant cell populations. Therefore, efficient anti-cancer therapy depends on targeting cancer cells at all stages of differentiation.

EMT has been suggested as the critical step in tumor cell dissemination and particularly associates with resistance towards chemotherapy and immunotherapy [1]. Here we established and characterized the first human cellular model of EMT in HCC progression allowing us to determine drug efficacy of novel and currently approved anti-cancer agents. Our data revealed that epithelial cells are more sensitive to the targeted therapeutic agents such as sorafenib and erlotinib, whereas mesenchymal cells show a more efficient susceptibility to chemotherapeutic drugs such as doxorubicin, cisplatin and epirubicin. Combined application of sorafenib and doxorubicin showed two advantages. Firstly, the effective concentration of drugs could be reduced and side effects could be minimized. Secondly, combined therapy is capable of targeting both, epithelial and mesenchymal cells, which might have the potential to reduce the risk of HCC recurrence. Yet, both cell lines showed no response against bevacizumab, referring to the limitation of the HCC model to study angiogenic mechanisms *in vitro*.

The efficacy of combining sorafenib and doxorubicin was shown in a phase II trial, resulting in increased overall and progression free survival in patients with advanced HCC compared to those who received a monotherapy with doxorubicin [21]. Furthermore, a phase III randomized study which compares sorafenib together with or without doxorubicin treatment in advanced or metastatic liver cancer is currently recruiting HCC patients

(http://www.clinicaltrial.gov, NCT01015833). Other ongoing clinical trials investigate the combination of sorafenib and doxorubicin or other chemotherapeutics using TACE (NCT01011010, NCT00478374, NCT0085528).

Our data revealed a significant upregulation of SPARC in mesenchymal 3sp cells which has been reported in patient samples at advanced stages of disease [22]. The role of this protein in hepatocarcinogenesis, however, is rather ambiguous by acting either as a tumor promoter [23] or tumor suppressor [22]. Notably, we could show for the first time that SPARC is epigenetically upregulated in human HCC progression by demethylation. Further studies will reveal the consequences of SPARC overexpression in hepatocarcinogenesis. In the same line, CGH analysis revealed homozygous loss of the Wnt signaling component AXIN1 as well as of the cation-selective channel TRPM3. While deletion of TRPM3 has not been reported in cancer progression, AXIN1 was found to be mutated in 5-25% of HCC patients and associated with poor differentiation [24]. These findings show that our EMT model is genetically well defined and thus, particularly valid to study human HCC progression without unkown genetic variations in widely used human hepatoma cell lines.

Human models of hepatocellular EMT which reliably reflect HCC progression are invaluable tools in pre-clinical studies for (i) the identification of molecular mechanisms underlying HCC progression, (ii) the pharmacological determination of dose-effect relationships and thus the efficacy of single and combined treatments with novel and currently used therapeutic anti-cancer drugs, and (iii) the (re)-evaluation of drug target specificity and pleiotropic effects after drug application.

3.6. Acknowledgements

The authors who have taken part in this study declared that they do not have anything to declare regarding funding from industry or conflict of interest with respect to this manuscript. The authors are grateful to Maria Eisenbauer for excellent technical assistance in cell culture. This work was supported by the European Union, FP7 Health Research, project number HEALTH-F4-2008-202047 and by the Austrian Science Fund, FWF, grant numbers P19598-B13 and P20905-B13.

3.7. References

[1]Thiery JP, Acloque H, Huang RY, Nieto MA. Epithelial-mesenchymal transitions in development and disease. Cell 2009;139:871-890.

[2]Yang J, Weinberg RA. Epithelial-mesenchymal transition: at the crossroads of development and tumor metastasis. Dev Cell 2008;14:818-829.

[3]Huber MA, Kraut N, Beug H. Molecular requirements for epithelial-mesenchymal transition during tumor progression. Curr Opin Cell Biol 2005;17:548-558.

[4]Giannelli G. The epithelial-mesenchymal transition: fact or fiction in cancer? Hepatology 2009;50:1344-1346.

[5]van Zijl F, Zulehner G, Petz M, Schneller D, Kornauth C, Hau M, et al. Epithelial-mesenchymal transition in hepatocellular carcinoma. Future Oncol 2009;5:1169-1179.

[6]Yang MH, Chen CL, Chau GY, Chiou SH, Su CW, Chou TY, et al. Comprehensive analysis of the independent effect of twist and snail in promoting metastasis of hepatocellular carcinoma. Hepatology 2009;50:1464-1474.

[7]Yuki K, Hirohashi S, Sakamoto M, Kanai T, Shimosato Y. Growth and spread of hepatocellular carcinoma. A review of 240 consecutive autopsy cases. Cancer 1990;66:2174-2179.

[8]Parkin DM, Bray F, Ferlay J, Pisani P. Global cancer statistics, 2002. CA Cancer J Clin 2005;55:74-108.

[9]Roxburgh P, Evans TR. Systemic therapy of hepatocellular carcinoma: are we making progress? Adv Ther 2008;25:1089-1104.

[10]Bruix J, Llovet JM. Major achievements in hepatocellular carcinoma. Lancet 2009;373:614-616.

[11]Llovet JM, Bruix J. Novel advancements in the management of hepatocellular carcinoma in 2008. J Hepatol 2008;48 Suppl 1:S20-S37.

[12]Bruix J, Sherman M. Management of hepatocellular carcinoma. Hepatology 2005;42:1208-1236.

[13]Llovet JM, Bruix J. Systematic review of randomized trials for unresectable hepatocellular carcinoma: Chemoembolization improves survival. Hepatology 2003;37:429-442.

[14]Marelli L, Stigliano R, Triantos C, Senzolo M, Cholongitas E, Davies N, et al. Treatment outcomes for hepatocellular carcinoma using chemoembolization in combination with other therapies. Cancer Treat Rev 2006;32:594-606.

[15]Cheng AL, Kang YK, Chen Z, Tsao CJ, Qin S, Kim JS, et al. Efficacy and safety of sorafenib in patients in the Asia-Pacific region with advanced hepatocellular carcinoma: a phase III randomised, double-blind, placebo-controlled trial. Lancet Oncol 2009;10:25-34.

[16]Finn RS. Development of molecularly targeted therapies in hepatocellular carcinoma: where do we go now? Clin Cancer Res 2010;16:390-397.

[17]Llovet JM, Ricci S, Mazzaferro V, Hilgard P, Gane E, Blanc JF, et al. Sorafenib in advanced hepatocellular carcinoma. N Engl J Med 2008;359:378-390.

[18]Sagmeister S, Eisenbauer M, Pirker C, Mohr T, Holzmann K, Zwickl H, et al. New cellular tools reveal complex epithelial-mesenchymal interactions in hepatocarcinogenesis. Br J Cancer 2008;99:151-159.

[19]van Zijl F, Mair M, Csiszar A, Schneller D, Zulehner G, Huber H, et al. Hepatic tumor-stroma crosstalk guides epithelial to mesenchymal transition at the tumor edge. Oncogene 2009;28:4022-4033.

[20]Heldin CH, Ostman A, Ronnstrand L. Signal transduction via platelet-derived growth factor receptors. Biochim Biophys Acta 1998;1378:F79-113.

[21]Keating GM, Santoro A. Sorafenib: a review of its use in advanced hepatocellular carcinoma. Drugs 2009;69:223-240.

[22]Atorrasagasti C, Malvicini M, Aquino JB, Alaniz L, Garcia M, Bolontrade M, et al. Overexpression of SPARC obliterates the in vivo tumorigenicity of human hepatocellular carcinoma cells. Int J Cancer, 2009/10/16 ed; 2010. p. 2726-2740.

[23]Le Bail B, Faouzi S, Boussarie L, Guirouilh J, Blanc JF, Carles J, et al. Osteonectin/SPARC is overexpressed in human hepatocellular carcinoma. J Pathol 1999;189:46-52.

[24]Imbeaud S, Ladeiro Y, Zucman-Rossi J. Identification of novel oncogenes and tumor suppressors in hepatocellular carcinoma. Semin Liver Dis 2010;30:75-86.

3.8. Figure legends

Fig. 1. Epithelial and mesenchymal characteristics of 3p and 3sp HCC cells. (A) Phase contrast images display an epithelial (3p) and a fibroblastoid phenotype of 3sp cells (bar, 50 µm). (B) qRT-PCR analysis of epithelial (E-cadherin, keratin 8) and mesenchymal markers (LEF1, SNAI1, SNAI2 and ZEB1) in 3p and 3sp cells. (C) Confocal immunofluorescence analysis of the epithelial markers E-cadherin, β-catenin, p^{120}catenin and keratin 8 as well as the mesenchymal marker vimentin. Localization of actin at cell membranes and as stress fibers as indicated by phalloidin staining (red). Nuclei were counterstained with To-Pro3 (blue). Bar, 25 µm. dCT, delta CT value.

Fig. 2. Mesenchymal 3sp HCC cells exhibit enhanced migration and invasion. (A) Proliferation kinetics of epithelial 3p and mesenchymal 3sp cells. (B) Migration assay using the Platypus® technology after 3 days (C) Quantification of cell migration by fluorometric analysis. (D) Invasion assays employing the Platypus® technology after 7 days. Upper panel and lower panel show the invasion area in the absence and presence of the mask, respectively. (E) Quantification of cell invasion by fluorometric analysis. Cells were visualized with green CellTracker™. Bar, 250 µm; ***, p<0,005.

Fig. 3. Mesenchymal 3sp HCC cells derived from epithelial 3p HCC cells through EMT *in vivo*. CGH analysis revealed a homozygous loss of genomic DNA in 3p and 3sp cells. (A) Homozygous loss of DNA in the TRPM3 and (B) AXIN1 gene locus. Red bars indicate exons and blue bars denote the positions of arrayed oligonucleotides on the chromosome. bps, basepairs.

Fig. 4. Global transcriptome analysis shows regulation of EMT-specific genes in 3sp HCC cells. Gene Set Enrichment Analysis of a whole-genome Affymetrix GeneChip® was performed. (A) Downregulation (blue) of epithelial markers and (B) upregulation (red) of EMT regulators in 3sp cells were determined. The -fold upregulation of mRNA was calculated and depicted by the ratio of (A) 3p to 3sp cells (3p/3sp) and of (B) 3sp to 3p cells (3sp/3p). (C) DNA methylation testing by qPCR upon methylation-sensitive digestion shows demethylation of the SPARC promoter in 3sp cells. 4 replicates of each cell type were analyzed. DNA from male (n=4) and female (n=4) blood were used as negative controls. (D) Confirmation of SPARC upregulation in 3sp cells by qRT-PCR. dCT, delta CT value. ACTA2, smooth muscle actin; CDH1, E-cadherin; CLDN, claudin; CTGF, connective tissue growth factor; DDR2, discoid domain receptor; DSP, desmoplakin; EPCAM, epithelial cellular adhersion molecule; FAP; fibroblast activation protein; HNF4A, hepatocyte nuclear factor 4α; KRT, keratin; LEF1, lymphoid enhancing factor 1; LOX, lysyl oxidase; MMP, matrix metalloproteinase; PDGF-Rβ, platelet-derived growth factor receptor β; SNAI2, Slug; SPARC, secreted protein, acidic, cystein-rich; TGF-β, transforming growth factor-β; TNC, tenascin C; VIM, vimentin.

Fig. 5. Mesenchymal 3sp HCC cells respond to cytostatic agents rather than to targeted therapeutic drugs. Cytotoxicity of anti-cancer agents was analyzed by MTT assays and IC_{50} values were calculated. Dose-response relationships of 3p and 3sp cells were compared. Red dotted lines indicate IC_{50}.

Fig. 6. Combined treatment with sorafenib and doxorubicin efficiently targets both, epithelial and mesenchymal HCC cells. Combined application was performed by delivering cells with one drug in increasing concentrations while the second drug was kept constant at the IC_{50} concentration**.** Dose response relationships for 3p and 3sp cells upon (A) treatment

with doxorubicin alone or in combination with sorafenib (+ IC_{50} sora) and (C) sorafenib alone or in combination with doxorubicin (+ IC_{50} doxo) are shown. The resulting change of IC_{50} values (arrow, %) of single to combined treatment are depicted for (B) doxorubicin and (D) sorafenib.

Figure 1

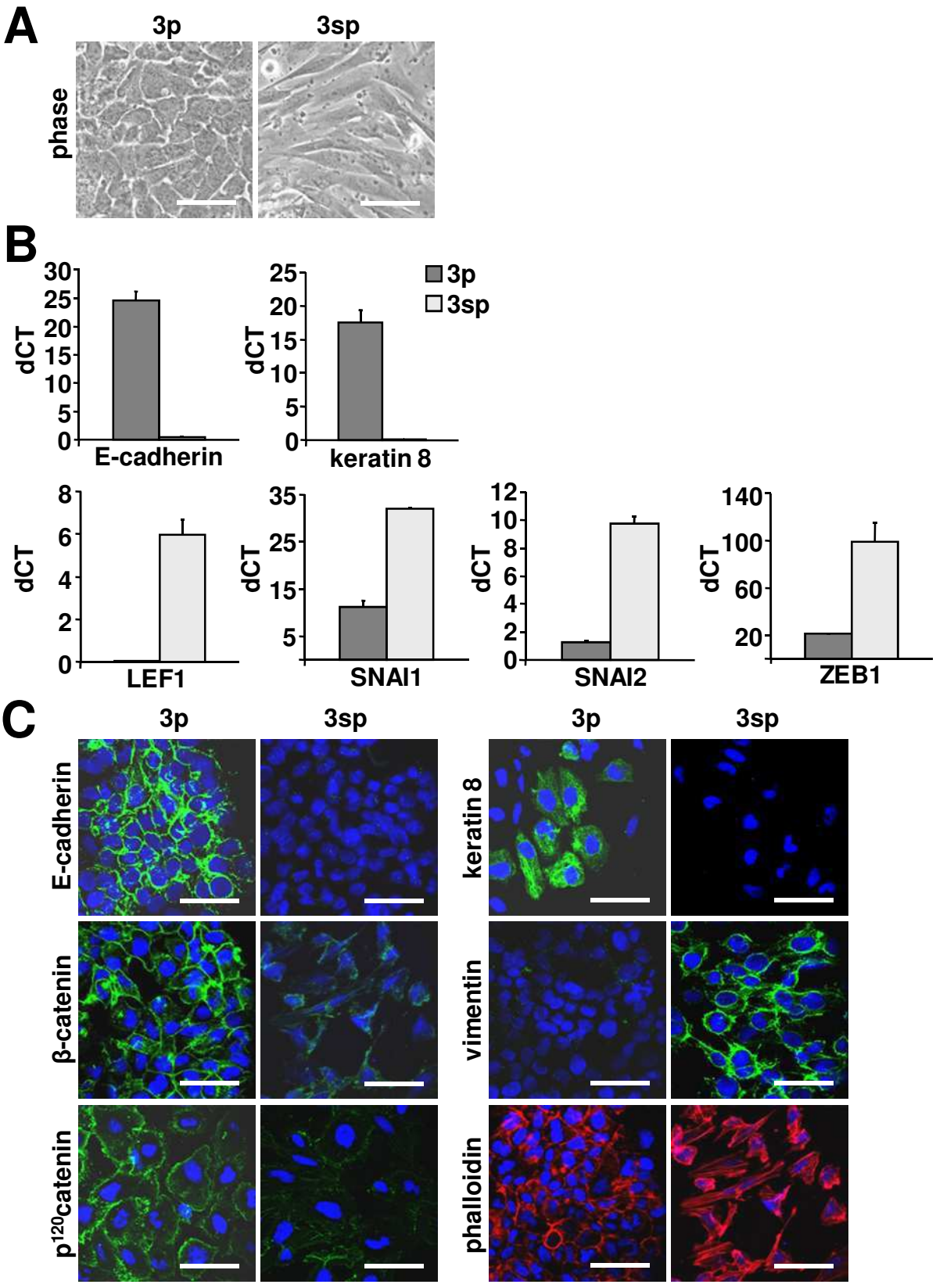
A
3p
3sp
phase
B
dCT
E-cadherin
keratin 8
3p
3sp
LEF1
SNAI1
SNAI2
ZEB1
C
3p
3sp
E-cadherin
keratin 8
β-catenin
vimentin
p120catenin
phalloidin

Figure 2

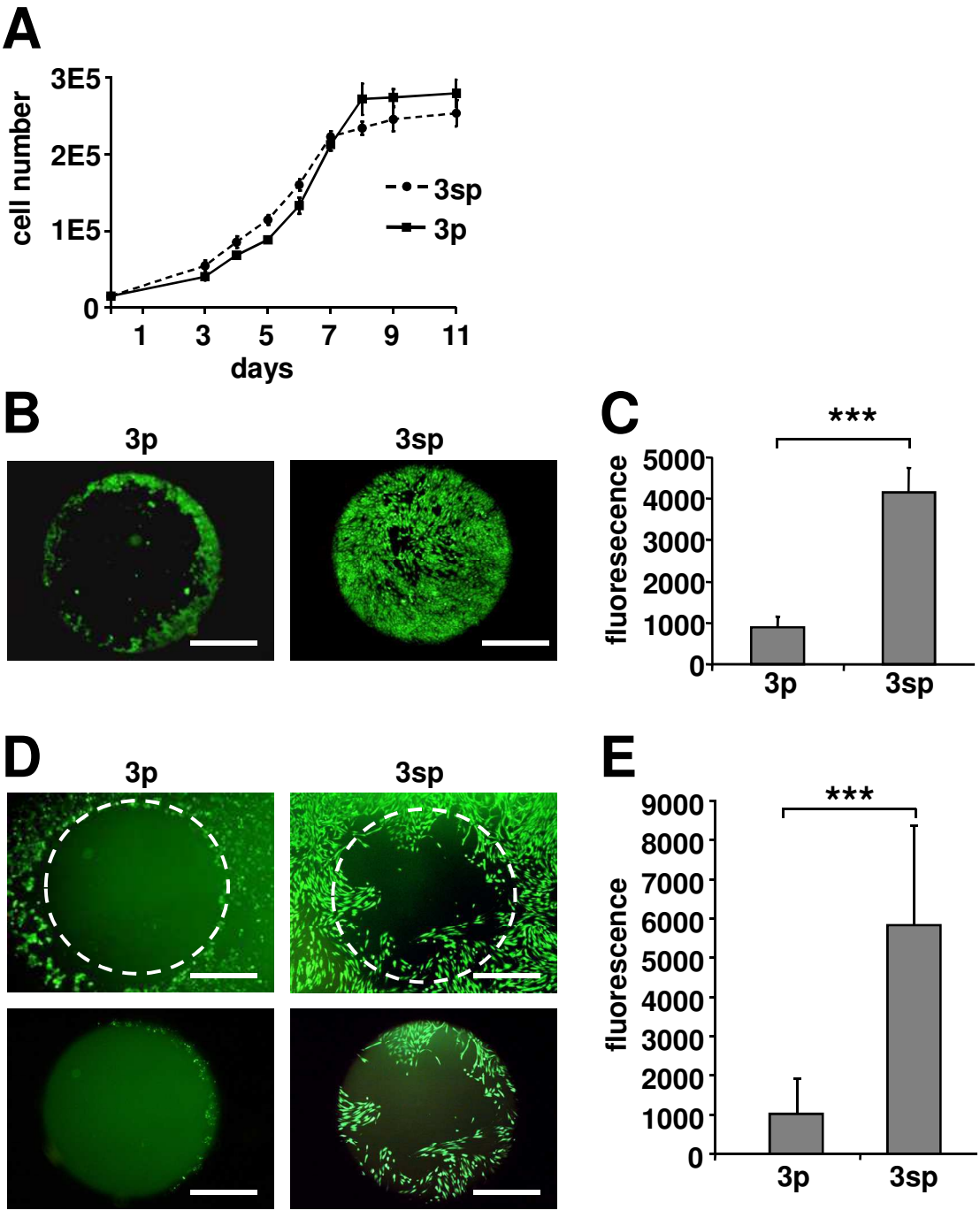
A
3E5
2E5
1E5
0
cell number
1
3
5
7
9
11
days
3sp
3p
B
3p
3sp
C
***
5000
4000
3000
2000
1000
0
fluoresecence
3p
3sp
D
3p
3sp
E
***
9000
8000
7000
6000
5000
4000
3000
2000
1000
0
fluorescence
3p
3sp

Figure 3

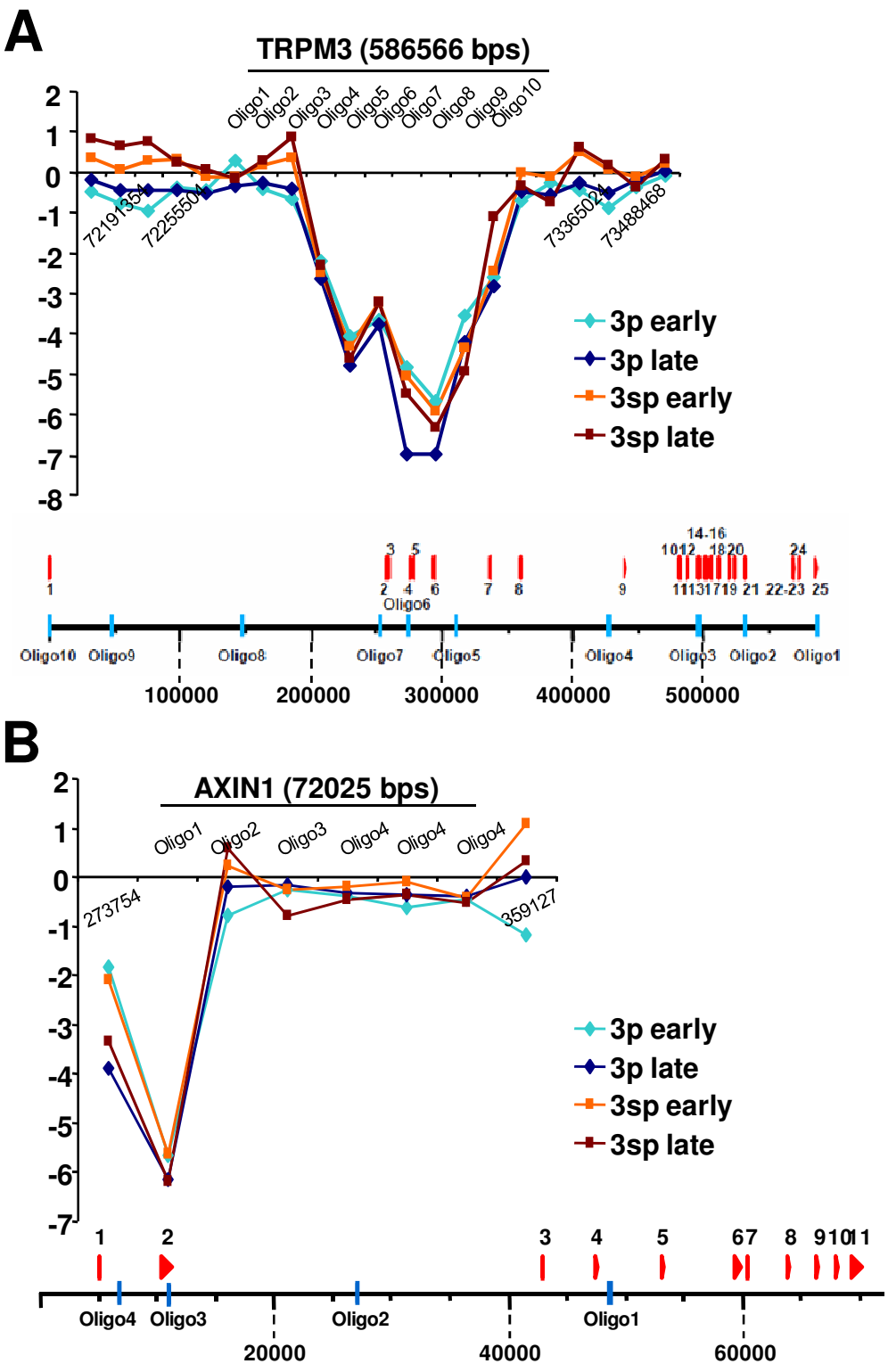
A
TRPM3 (586566 bps)
Oligo1 Oligo2 Oligo3 Oligo4 Oligo5 Oligo6 Oligo7 Oligo8 Oligo9 Oligo10
7219354
7225550
7336502
7348846
3p early
3p late
3sp early
3sp late
Oligo10 Oligo9 Oligo8 Oligo7 Oligo5 Oligo4 Oligo3 Oligo2 Oligo1
100000 200000 300000 400000 500000
B
AXIN1 (72025 bps)
Oligo1 Oligo2 Oligo3 Oligo4 Oligo4 Oligo4
273754
359127
3p early
3p late
3sp early
3sp late
Oligo4 Oligo3 Oligo2 Oligo1
20000 40000 60000

Figure 4

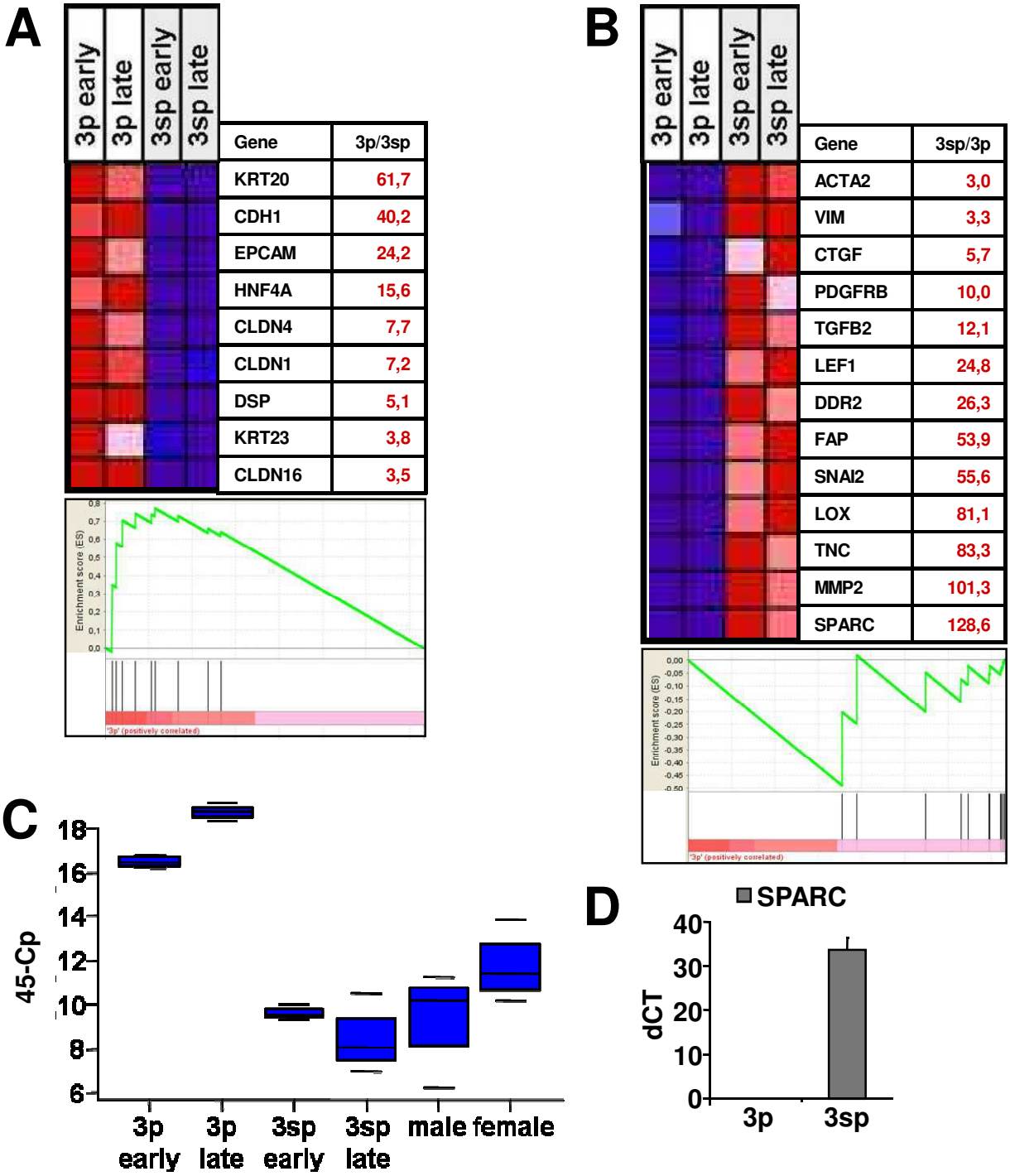
A
3p early
3p late
3sp early
3sp late
Gene
3p/3sp
KRT20
61,7
CDH1
40,2
EPCAM
24,2
HNF4A
15,6
CLDN4
7,7
CLDN1
7,2
DSP
5,1
KRT23
3,8
CLDN16
3,5
Enrichment score (ES)
'3p' (positively correlated)
B
3p early
3p late
3sp early
3sp late
Gene
3sp/3p
ACTA2
3,0
VIM
3,3
CTGF
5,7
PDGFRB
10,0
TGFB2
12,1
LEF1
24,8
DDR2
26,3
FAP
53,9
SNAI2
55,6
LOX
81,1
TNC
83,3
MMP2
101,3
SPARC
128,6
Enrichment score (ES)
'3p' (positively correlated)
C
45-Cp
18
16
14
12
10
8
6
3p early
3p late
3sp early
3sp late
male
female
D
SPARC
dCT
40
30
20
10
0
3p
3sp

Figure 5

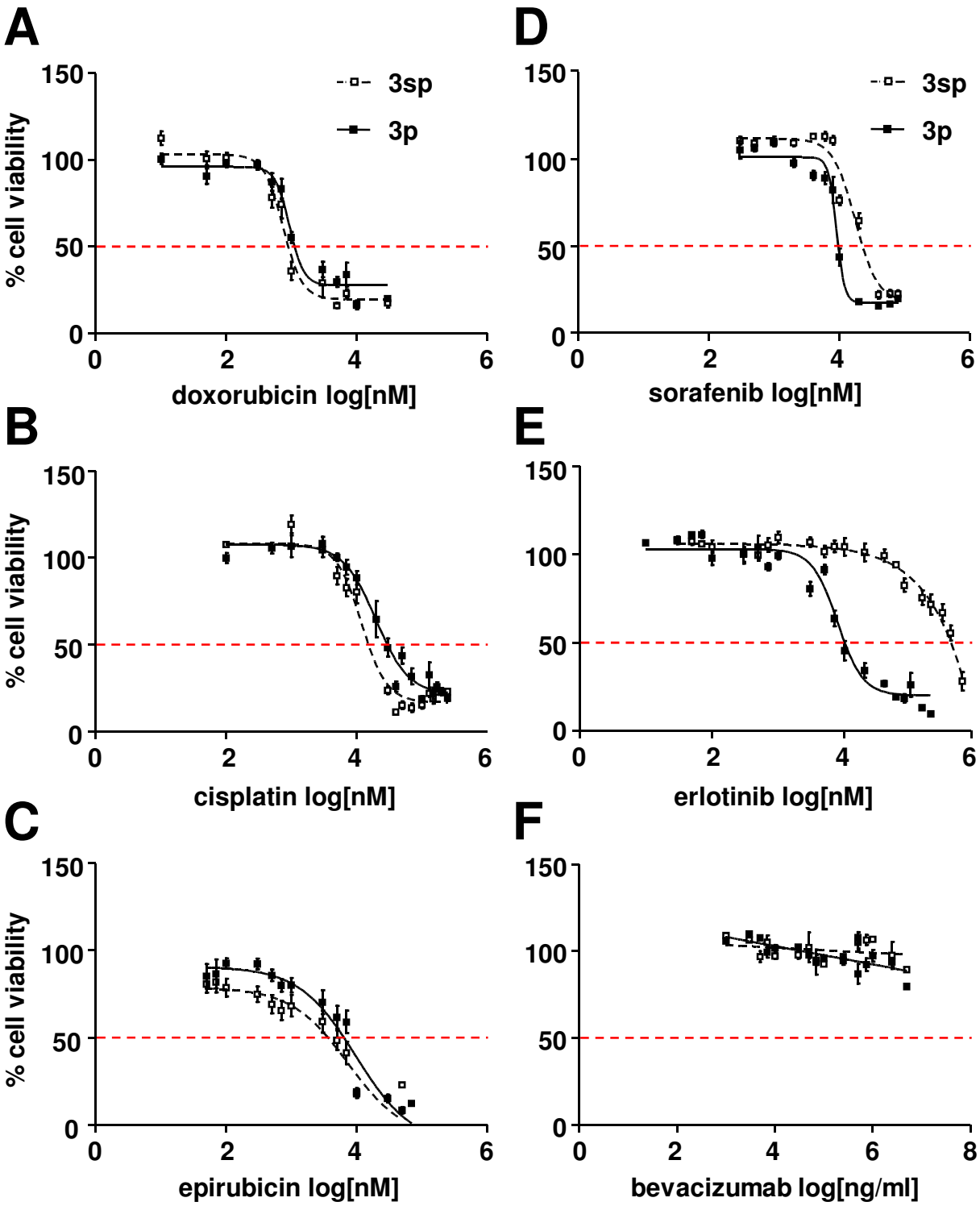
A
D
B
E
C
F
3sp
3p
% cell viability
doxorubicin log[nM]
sorafenib log[nM]
cisplatin log[nM]
erlotinib log[nM]
epirubicin log[nM]
bevacizumab log[ng/ml]
0
50
100
150
0
2
4
6
8

Figure 6

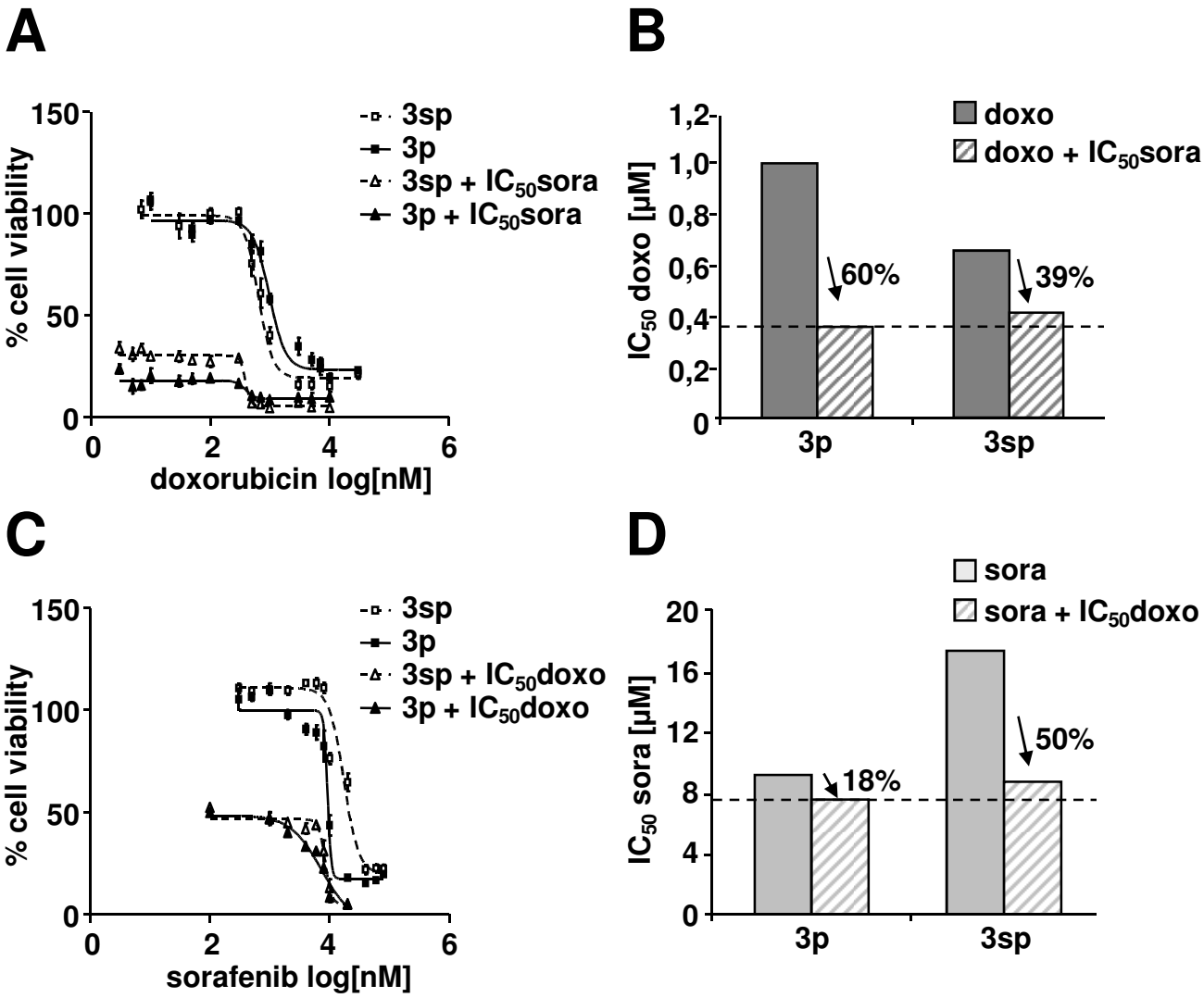
A
150
100
50
0
% cell viability
0
2
4
6
doxorubicin log[nM]
3sp
3p
3sp + IC50sora
3p + IC50sora
B
1,2
1,0
0,8
0,6
0,4
0,2
0
IC50 doxo [µM]
doxo
doxo + IC50sora
60%
39%
3p
3sp
C
150
100
50
0
% cell viability
0
2
4
6
sorafenib log[nM]
3sp
3p
3sp + IC50doxo
3p + IC50doxo
D
20
16
12
8
4
0
IC50 sora [µM]
sora
sora + IC50doxo
18%
50%
3p
3sp

Table 1. IC_{50} values of anti-cancer agents after single or combined therapeutic treatment of 3p and 3sp cells.

IC_{50} [µM]					
chemotherapeutics			**targeted therapeutic agents**		
drug	**3p**	**3sp**	**drug**	**3p**	**3sp**
cisplatin	19,01	10,14	erlotinib	14,30	399,23
epirubicin	9,79	7,66	bevacizumab	n.d.	n.d.
doxorubicin	0,98	0,65	sorafenib	9,27	17,54
doxorubicin (+ sorafenib)	0,39	0,39	sorafenib (+ doxorubicin)	7,63	8,83

n.d. not determined

3.10. Supplementary Material

Supplementary Material and Methods

Cell Culture

Human 3p and 3sp heptoma cells were cultured on plastic in RPMI supplemented with 10% fetal calf serum (FCS) and antibiotics, except that early 3p cells were grown on collagen-coated tissue culture plates in ACL-4 medium supplemented with 5% FCS. All cells were kept at 5% CO_2 and 37°C and routinely screened for the absence of mycoplasma,

Analysis of diploidy

Cells were trypsinized, washed with PBS and 1 x 10^6 cells were incubated with 1 ml hypotonic DNA staining buffer containing 5mg/ml propidium iodide (Calbiochem, San Diego, CA, USA), 0,1% sodium citrate, 0,3% Triton X-100 and 20 µg/ml ribonuclease A (all from Sigma, St. Louis, MO, USA) for 30 minutes on 4°C in the dark. Determination of the DNA content was performed by flow cytometry (FACSCalibur, BD Biosciences, San Jose, CA, USA)

Short tandem repeat (STR) analysis

PCR of seven short tandem repeats (Supplementary Table 1) was performed to verify the genetic origin of human 3p and 3sp hepatoma cells.

3-dimensional (3D) spheroid formation of HCC cells

Spheroid formation and incubation was performed as described [1]. Briefly, a cell suspension of 3 x 10^2 3p cells per 100 µl or a 1:1 mixture of 3p and 3sp cells in RPMI containing 20% methyl cellulose (Sigma, St Louis, MO, USA) was incubated for 3 days at 37°C and 5% CO_2. After harvesting, 96 spheroids were mounted in collagen I (Sigma, St Louis, MO USA) and

plated into flexiPERM conA wells (Greiner Bio-One GmbH, Kremsmuenster, Austria) to harden at 37°C for 15 minutes. Gels were then transferred into a 24-well plate and incubated with medium at cell culture conditions as outlined. CellTracker™ (Green CMFDA; Invitrogen, Carlsbad, USA) was applied at a concentration of 5 µM before spheroid formation and incubated as outlined by the instructions of the manufacturer (Invitrogen, Eugene, Oregon, USA). The fluorescence signal was visualized by microscopy (Nikon, TE 300, Japan).

Confocal immunofluorescence microscopy of spheroids

Collagen gels were fixed in 4% formaldehyde/PBS for 10 minutes at room temperature. After blocking for 30 minutes (1% PBS/0.5% Tween 20/0.2% fish gelatine with 0.2 mg/ml IgG_1) at room temperature, the following primary antibodies were applied at a dilution of 1:100: anti-β-catenin (BD Transduction Laboratories, Lexington, UK), anti-E-cadherin (BD), anti-p^{120}catenin ($p120^{ctn}$; BD)), anti-keratin 8 (Progen, Heidelberg, Germany), Texas Red-X phalloidin (Invitrogen, Carlsbad, USA) and anti-vimentin (Sigma, Saint Louis, USA). The corresponding secondary antibody (Alexa 488; Invitrogen, Carlsbad, USA) was applied after one hour. Nuclei were visualized with To-Pro3 (Invitrogen, Carlsbad, USA) at a dilution of 1:10.000. Imaging was performed by confocal immunofluorescence microscopy (Zeiss, Jena, Germany).

Polymerase chain reaction (PCR) of genomic DNA

Chromosomal DNA was isolated with GenElute Mammalian Genomic DNA Miniprep Kit (Sigma; St Louis, MO, USA). PCR was performed using chromosomal DNA and illustra PuReTaq Ready-To-Go PCR beads (GE Healthcare, Buckinghamshire, UK) and 4 µM primer mix of following primers: human TRPM3: exon 1, forward (for) 5'-CAGGCAAGGCTACTTGACTA-3', reverse (rev) 5'-CACCAGCCTCTTGTCTCTGA-3';

exon 3, for 5'-GGTGGACGGAGAAGGGCAGGA-3', rev 5'-GGGGCAGGGGACTCAGAGCA-3'; exon 6, for 5'-CTCCTAGCTCCCCGCCACCA-3', rev 5'-TGCCAGTGGGAACAACCGCT-3'; exon 8, for 5'-TCCACAATTAGACATGACGCTGCAA-3', rev 5'-GCTGGCCACCCATGCGGAAT-3'; exon 9, for 5'-CCTGACTCATAGCAAGGGCCCCA-3', rev 5'-GCTGTCAGGATAGCCAAATCAATGTCC-3'; exon 10, for 5'-ATGCCTCGGCCCCAGACCAA-3', rev 5'-AGATGGCGCCTGCAGAGGGA-3'; exon 12, for 5'-TGAACTGCCCTCCACCAGCCA-3', rev 5'-GGTCAGTCAGGCAGCTCCCCA-3'; exon 15, for 5'-AGGACAGGAGCTGGCCTCGT-3', rev 5'-CCTGTGTGTGCATCACTGGGGT-3'; exon 18, for 5'-GCCTGGCCTTCCCAGGCTAC-3', rev 5'-TGGACGTTGGCTCCTTGTGGC-3'; exon 21, for 5'-TCCCTCTGCTTCCCCACCCT-3', rev 5'-TCAACACATGGCCCTGGGAGT-3'; exon 24, for 5'-TCTCTGCCACACCCCCAGCC-3', rev 5'-TCTGCAGGAGGCAGGTGTCCA-3'; exon 25, for 5'-CTCCTGCAGCCCCTGCCAAC-3', rev 5'-GGGAAGGCAGCTCTGTCCGC-3'. Human AXIN1: exon 1, for 5'-CCGGCTACCCGAGATACTCAGCA-3', rev 5'-GCTCCAGGCATCATGGCAGCAA-3'; exon 2, for 5'-CCCCCAGTGCCTGGTGAGGA-3', rev 5'-TGGGGCTCTCCGAGCCTGTC-3'; exon 3, for 5'-TCCTGGCGGGAGCCAGTCAA-3', rev 5'-CTGCACCAGCGTCGGCAGAA-3'; exon 4, for 5'-ACAGGCAGGCACAAGGAGGC-3', rev 5'-CCCTGCTGCCCTCAGGGACT-3'; exon 5, for 5'-GGCCGGACACGAAAAGGGGG-3', rev 5'-CATCAGGACATCCCGGCGGC-3'; exon 6, for 5'-CGGCGATCCATCGTCAGGGC-3', rev 5'-GCGAGGCCATCACTGGCGTT-3'; exon 7, for 5'-AGGATGCGGAGAAGAACCAG-3', rev 5'-AGAAGTGCTCACGCTACACA-3'; exon 8, for 5'-ACGAGGAAGCCACAGCCCCA-3', rev 5'-TGCCTCCAGGACCTCTGCCC-3'; exon 9, for 5'-AGACCGAGTTGCCACGCACG-3', rev 5'-CCGGGAGGACCCTCAGGACG-3'; exon 10, for 5'-

TGAGGCCAGCAGGAGGGACC-3', rev 5'-GGGCCGAAAGCCTGATGCCA-3'; exon 11, for 5'-GGCCGTCCTGCCCGTCTTTG-3', rev 5'-GGCTGGAGGCAGGTGCAGTG-3'.

Verification of IC_{50} values by proliferation

6 x 10^4 cells /well were seeded in triplicates on collagen-coated 12-well plates and incubated with drugs at a concentration of determined IC_{50} values for 3 days. Cells were trypsinized and counted with a cell counter (CASY, Roche, Basel, Switzerland). Untreated cells were used as reference to calculate the percentage of proliferation.

Comparative genomic hybridization (CGH)

Male reference DNA (Promega, Madison, USA) and sample DNA were digested with AluI and RsaI (Promega, Madison, USA) and labeled by random priming with Cyanine 3- and Cyanine 5-dUTP (Perkin-Elmer, Massachusetts, USA), respectively, by using the BioPrime Array CGH Genomic Labeling Kit (Invitrogen, Carlsbad, USA). After purification with Microcon YM-30 filter units (Millipore, Billerica, USA), the two labeled DNA species were hybridized together with human cot-DNA (Roche, Basel, Switzerland) onto CGH arrays for 48 hours at 65°C. Slides were scanned with a G2505B Micro Array Scanner (Agilent, Santa Clara, USA). Feature extraction and data analysis were performed using the Feature Extraction and DNA Analytics software (Agilent, Santa Clara, USA), respectively.

Analysis of CpG methylation

600 ng genomic DNA of 3p and 3sp HCC cells and from pimary peripheral blood cells were digested with methylation-sensitive restriction enzymes (MSRE) overnight at 37°C by employing a mixture of 6 units of each AciI (New England Biolabs, Frankfurt am Main, Germany), Hin6I (Fermentas, St. Leon-Rot, Germany) and HpaII (Fermentas). Quantitative polymerase chain reaction (qPCR) was performed on MSRE-digested DNA covering the CpG

rich area at chr5:151,066,289-151,066,501 (human genome annotation: hg 19), including part of the first gene coding exon. This sequence region contains 9 MSRE sites when using the mixture of 3 enzymes mentioned above. Completion of digestion was confirmed using a control PCR covering known differentially methylated regions (DMRs; H19, IGF2, ABL1, PITX2, XIST and FMR1) as published recently [2]. 10 ng of MSRE-digested DNA was amplified in 10 µl PCR volume using 0.3 U HotStarTaq polymerase and buffer containing 1.5 mM $MgCl_2$ (Qiagen, Hilden, Germany) using a 384-well format and the LightCycler® LC480 (Roche, Vienna, Austria). Cycling was performed with 15 minutes of initial denaturation followed by 50 cycles with each 95°C for 40 sec, 65°C for 40 sec and 72°C for 80 sec including a final extension at 72°C for 7 minutes. A melting curve analysis was performed for confirming specificity of amplicons with a Tm of 88.4°C ±0.6°C. Cp values were extracted from qPCR-data using the LigthCycler LC480 software. Boxplots were generated from quadruplicate "45-Cp" values using R statistical software.

References

[1]van Zijl F, Mair M, Csiszar A, Schneller D, Zulehner G, Huber H, et al. Hepatic tumor-stroma crosstalk guides epithelial to mesenchymal transition at the tumor edge. Oncogene 2009;28:4022-4033.

[2]Weinhaeusel A, Thiele S, Hofner M, Hiort O, Noehammer C. PCR-based analysis of differentially methylated regions of GNAS enables convenient diagnostic testing of pseudohypoparathyroidism type Ib. Clin Chem 2008;54:1537-1545.

Supplementary Figure legends

Supplementary Fig. 1. Human 3p and 3sp hepatoma cells are diploid. Flow cytometry analysis of cells stained with propidium iodide indicates diploid DNA content of (A) early and (B) late 3p cells as well as (C) early and (D) late 3sp cells.

Supplementary Fig. 2. Cell invasion of mesenchymal 3sp cells in 3-dimensional (3D) co-cultured 3p/3sp-derived spheroids. (A) 3p cells form compact and round spheroids which are unable to invade into the surrounding collagen gel. Co-cultivation of epithelial 3p and mesenchymal 3sp cells (3p + 3sp) showed spheroid formation and strong invasion into the gel (bar, 250 µm). (B) Staining of co-cultivated spheroids with CellTracker™ revealed that only mesenchymal 3sp cells (green) invade into the gel, while epithelial 3p cells (red) reside in the center of the spheroid (bar, 250 µm). (C) Immunofluorescence staining of membrane-bound β-catenin and E-cadherin showing the epithelial organization of 3p cells in a 3D setting, while detached mesenchymal 3sp cells (white arrows) from a co-cultivated spheroid lose these epithelial markers (bar, 25 µm).

Supplementary Fig. 3. Identification of chromosomal break points in TRPM3 and AXIN1. PCR discloses chromosomal breaks of (A) TRPM3 between exon 12 and exon 15 and of (B) AXIN1 between exon 2 and exon 3 in 3p and 3sp cells. Genomic DNA of primary human hepatocytes (prim hep) were used as control. Ex, exon; bp, 100 basepair ladder.

Supplementary Fig. 4. Downregulation of liver specific genes in 3sp HCC cells. Gene Set Enrichment Analysis (GSEA) of a whole-genome Affymetrix GeneChip® revealed downregulation of liver-specific genes in 3sp cells. Blue and red indicates down- and upregulation, respectively.

Supplementary Fig. 5. Sorafenib efficiently blocks cell migration of mesenchymal 3sp HCC cells. (A) Verification of calculated IC_{50s} by viability assays. Incubation of 3p and 3sp cells with drugs at their determined IC_{50} results in a reduction of viable cells to 50%. (B) Migration assays using the Platypus® technology shows movement of mesenchymal 3sp cells into the detection zone after 3 days. Treatment of doxorubicin at the IC_{50} shows a reduction of the cell number but no impaired migration, whereas treatment of sorafenib at the IC_{50} leads to a significantly reduced migratory potential of 3sp cells. (C) Quantification of 3sp cell migration by fluorometric analysis. Cells were visualized with green CellTracker™. Bar, 250 µm; ***, p<0,005.

Supplementary Figure 1

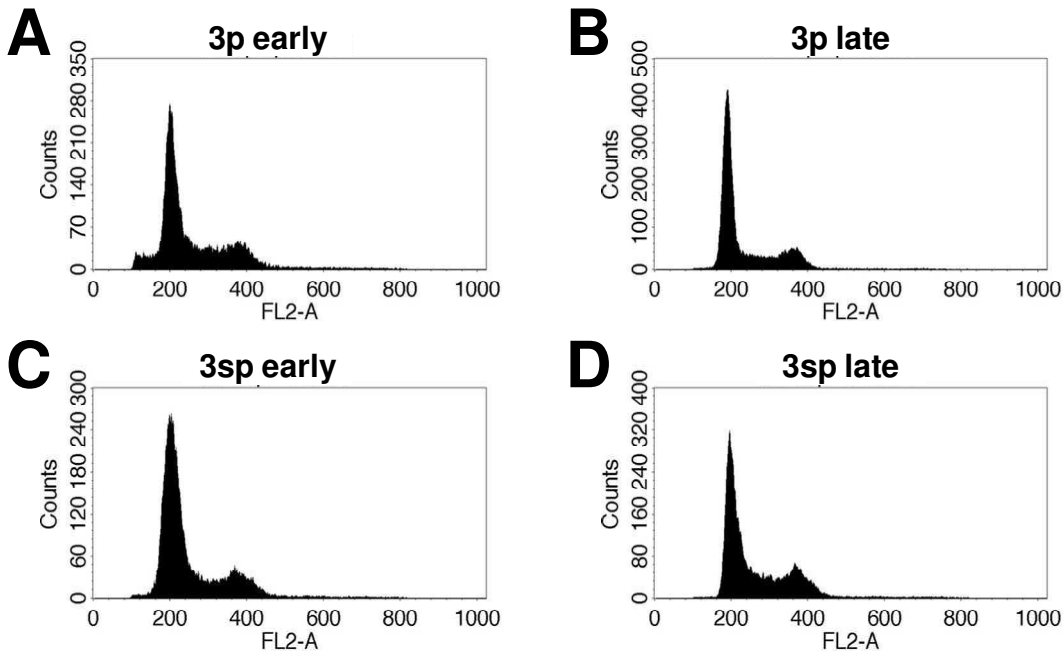

Supplementary Figure 2

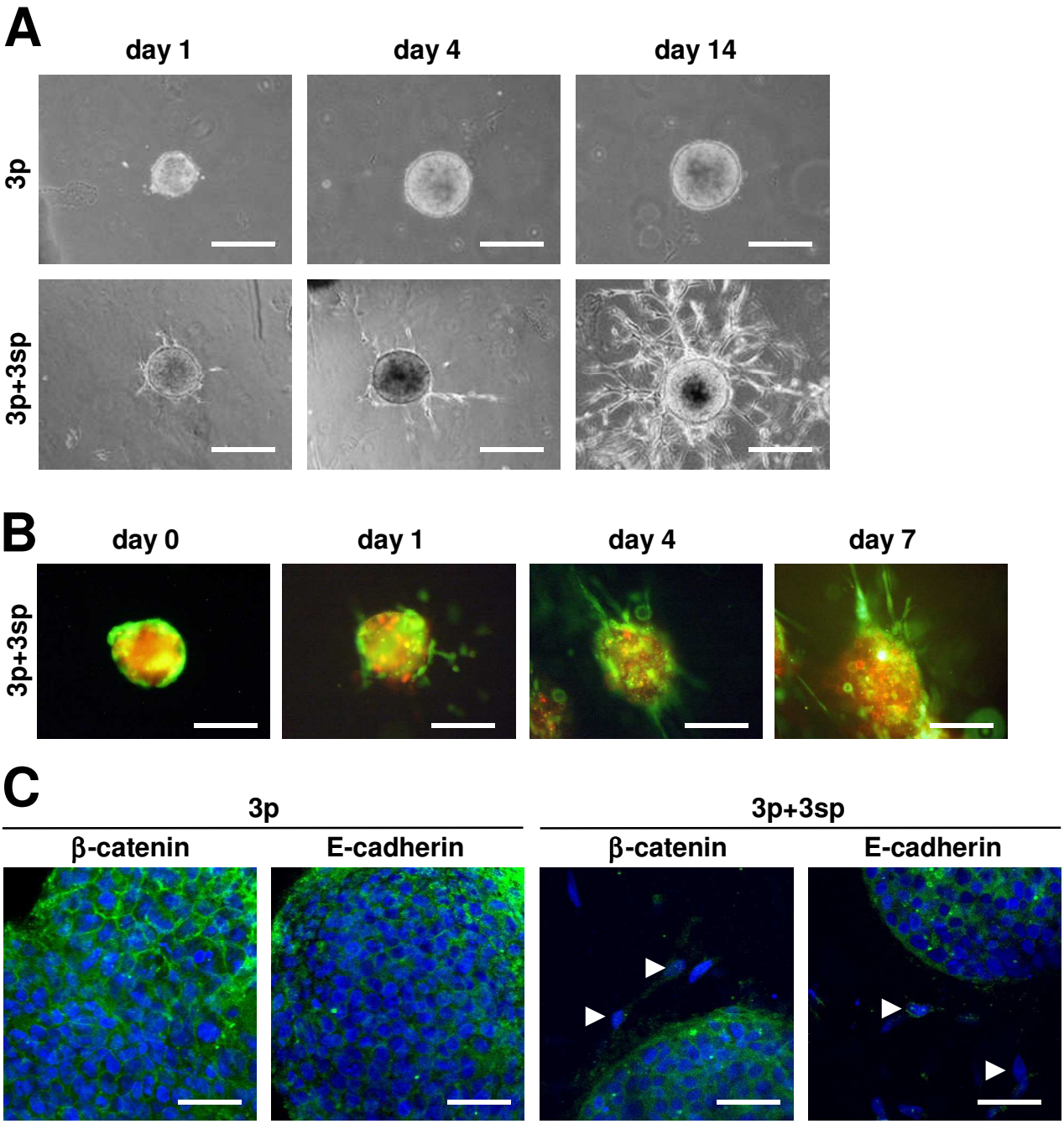

Supplementary Figure 3

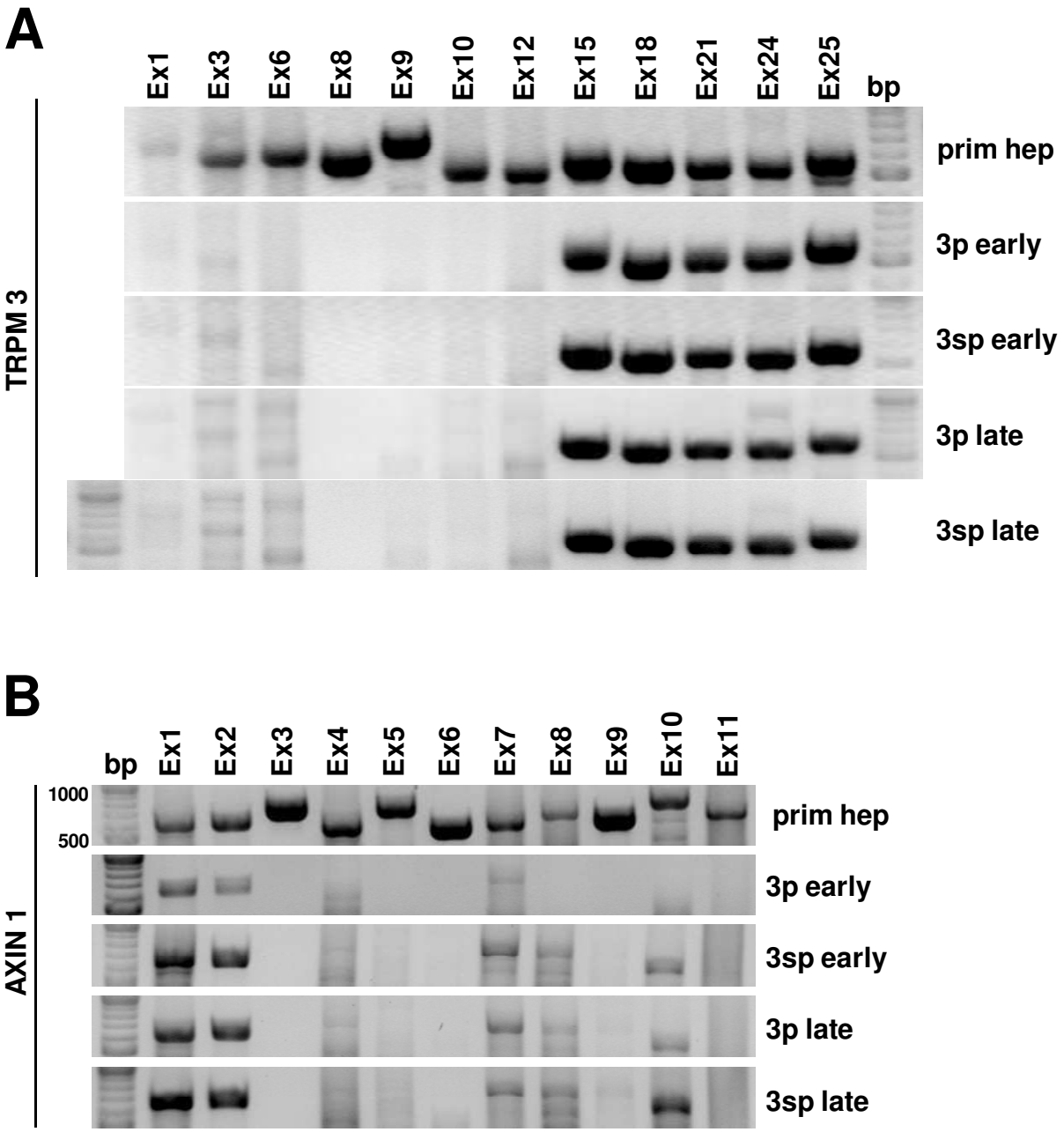

Supplementary Figure 4

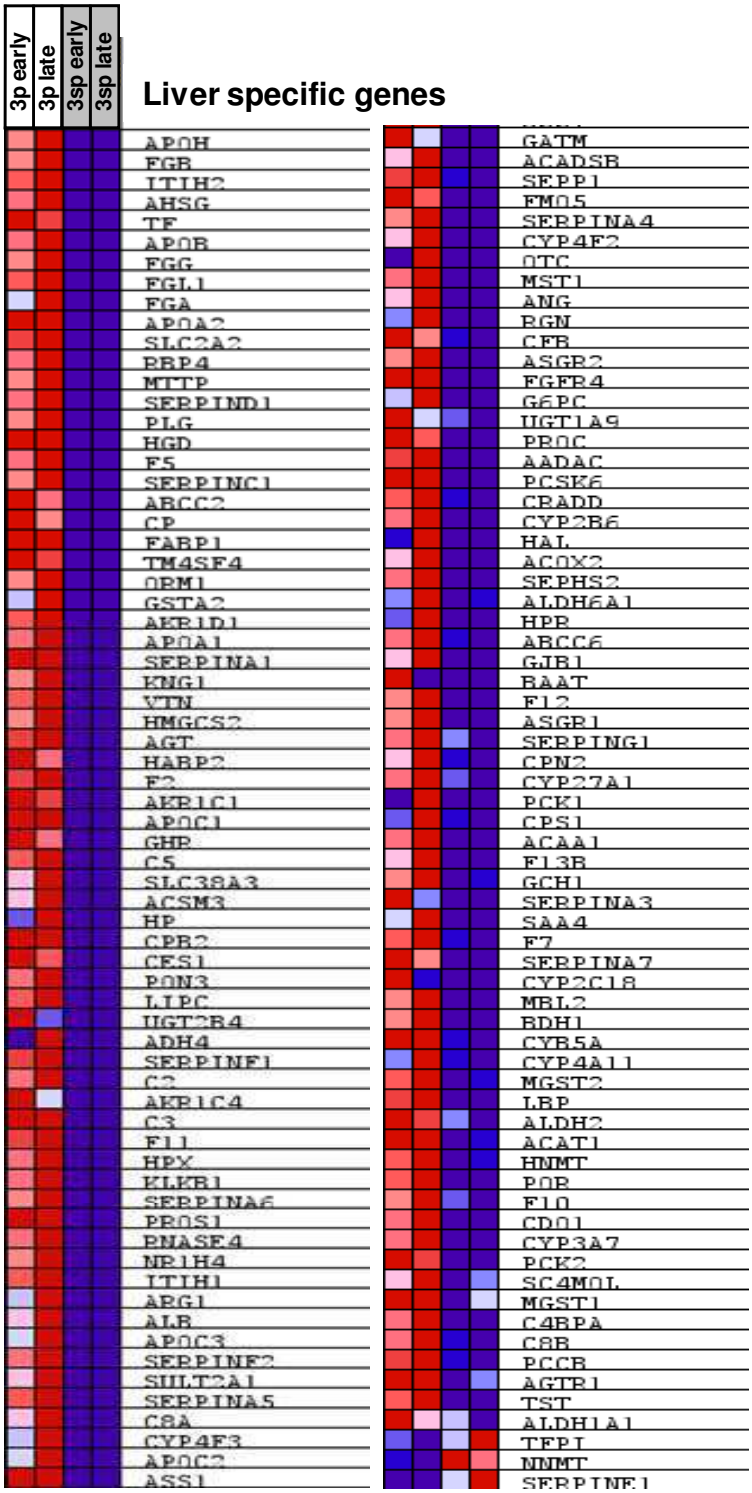

Supplementary Figure 5

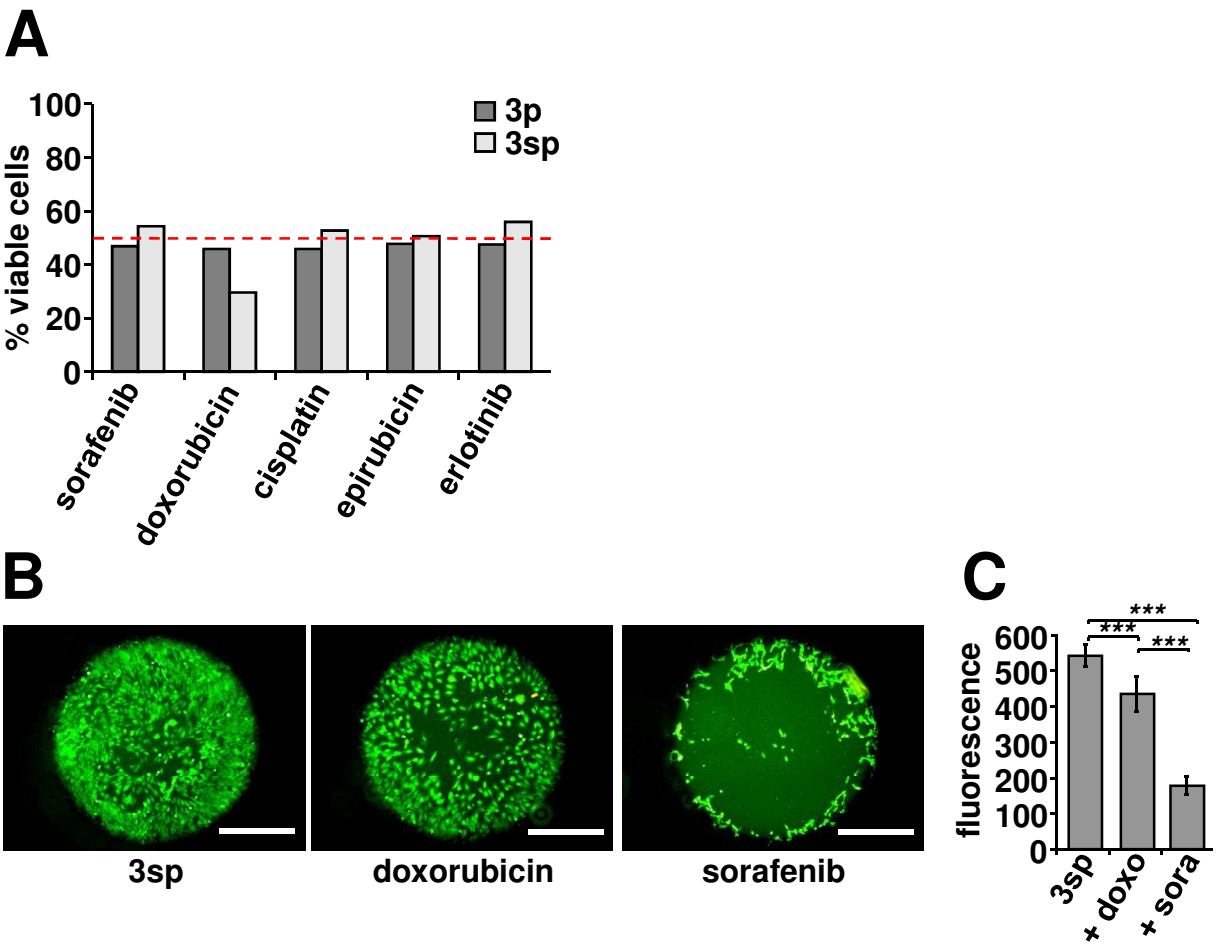

Supplementary Table 1. Primer for quantitative Real Time PCR

gene	forward primer	reverse primer
RhoA	CCATCATCCTGGTTGGGAAT	CCATGTACCCAAAAGCGC
E-cadherin	ACCACCTCCACAGCCACCGT	GCCCACGCCAAAGTCCTCGG
K8	AGGAGGCCGCTATGCAGGGT	GCTGGAGGCATGGGCAAGGG
LEF1	ACCCCACCTCTTGGCTGGCA	TGTGGGGACCAGGAGGACCG
SNAI1	GGCCCACCTCCAGACCCACT	CTCGAGGGTCAGCGGGGACA
SNAI2	GTCCGTCTGCCGCACCTGAG	CAGGAAGGAGCGCGGCATCT
ZEB1	CGTGGCCATTGCTGACCAGA	TTGGACTGCAGGGCTGACCG
ZEB2	GCCGAGTCCATGCGAACT	AATGAAGCAGCCGATCATGG

Abbreviation: Keratin 8, Lymphoid enhancer binding factor (LEF)1, Snail (SNAI1), Slug (SNAI2), Zinc finger E-box binding homeobox (ZEB)1 and 2.

Supplementary Table 2. Short tandem repeat analysis of 3p and 3sp HCC cells.

3p	3sp	marker	location	primer pair
338,346	**338,346**	CSF1PO	5q33.1	CCGGAGGTAAAGGTGTCTTAAAGT ATTTCCTGTGTCAGACCCTGTT
198,000	**198,000**	D13S317	13q.31.1	ATTACAGAAGTCTGGGATGTGGAGGA GGCAGCCCAAAAAGACAGA
152,000	**152,000**	vWA	12p13.31	GCCCTAGTGGATGATAAGAATAATCAGTATGTG GGACAGATGATAAATACATAGGATGGATGG
223,230	**223,230**	D7S820	7q.21.11	ATGTTGGTCAGGCTGACTATG GATTCCACATTTATCCTCATTGAC
270,274	**271,000**	TPOX	2p25.3	GCACAGAACAGGCACTTAGG CGCTCAAACGTGAGGTTG
130,142	**130,142**	D5S818	5q23.2	GGTGATTTTCCTCTTTGGTATCC AGCCACAGTTTACAACATTTGTATCT
282,000	**282,000**	D16S539	16q24.1	GGGGGTCTAAGAGCTTGTAAAAAG GTTTGTGTGTGCATCTGTAAGCATGTATC

4. Abbreviations

α-SMA	alpha smooth muscle actin
Akt	V-Akt murine thymoma viral oncogen homolog
ARHGEF9	Rho guanine nucleotide exchange factor 9
AXIN1	Axis inhibitor 1
BCLC	Barcelona Clinic Liver Cancer Classification
bHLH	basic helix loop helix
CCDN1	cyclin D1
Cdc42	cell division cycle 42
CDH1	cadherin 1
CDH1L	chromodomain helicase/ATPase DNA binding protein 1 like gene
CGH	comparative genomic hybridisation
CLT	cadaveric liver transplantation
CTGF	connective tissue growth factor
DEB	drug eluting beads
DNA	deoxyribonucleic acid
ECOG	Eastern Cooperative Oncology Group
EGF	epidermal growth factor
EGFR	epidermal growth factor receptor
EIF5A2	eukaryotic initiation factor 5A2
EMT	epithelial to mesenchymal transition
ErbB	avian erythoblastic leukemia viral oncogene homolog
Erk	extracellular signal regulated kinase
FOXC2	forkhead box C2
FSP-1	fibroblast-specific protein 1

HBV	Hepatitis B Virus
HCC	hepatocellular carcinoma
HCV	hepatitis C virus
HGF	hepatocyte growth factor
IC_{50}	half maximal inhibitory concentration
IFN	interferon
IGF	insulin-like growth factor
IGF1-R	insulin like growth factor 1 receptor
LDLT	living donor liver transplantation
LEF	lymphoid enhancer binding factor
Ln-5	Laminin – 5
MAPK	mitogen activated protein kinase
Mdm2	mouse double minute 2 homolog
MET	mesenchymal to epithelial transition
Met	oncogene Met
miRNA	micro ribonucleic acid
mTOR	mammalian target of Rapamycin
MUC1	mucin 1, cell surface associated
$p14^{ARF}$	cyclin-dependent kinase inhibitor 2A
PAR6A	partitioning defective protein 6
PCR	polymerase chain reaction
PDGFR	plateled-derived growth factor receptor
PEI	percutaneous ethanol injection
PI3K	phoshoinositide 3 Kinase
PTEN	phosphatase and tensin homolog
Raf	v-Raf 1 murine leukemia viral oncogene homolog

Ras	rat sarcoma viral oncogene
Rb	Retinoblastoma
RCTs	randomized controlled trials
RF	radiofrequency ablation
RhoB	Ras homolog gene family B
RPS6	ribosomal protein S6
SIP1	survival of motor neuron protein interacting protein 1
siRNA	small interfering ribonucleic acid
Smad	Mothers against Decapentaplegic
snRNA	small nucleolar ribonucleic acid
SPARC	secreted protein, acidic, rich in cystein
STAT1	signal transducer and activator of transcription 1
STR	short tandem repeats
TACE	transarterial chemoembolization
TAE	transarterial embolization
TGF-β	transforming growth factor – β
TGFβRI	transforming growth factor receptor I
TNM	Tumor – Node – Metastasis classification
UICC	International Union against Cancer
VEGFR	vascular endothelial growth factor receptor
Wnt	Wingless type MMTV integration type family
ZEB	zinc finger E-box binding homeobox
ZIP1	Smad interacting protein
ZO-1	zonula occludens – 1

5. Acknowledgements

First of all, I want to thank Wolfgang for giving me the opportunity to do my diploma thesis in his lab. Further thanks should go to all group members Franziska, Georg, Markus, Michi, Heidi, Doris and Alex for their very helpful support in experimental as well as theoretical questions but also interesting discussions and the funny friday evenings and festivities. Not to forget, thanks to Georg for teaching me ‘Wienerisch’ and being a great lunch deliverer as well as to Markus for his words of encouragement. An especial thank goes to Franziska, in her I found not only a very competent and patient supervisor but also a good friend. I learned so much from her and she always helped and supported me not only in questions regarding research. Without her collaboration this work wouldn’t be possible.

I also wish to acknowledge my parents for the financial support and their strong believe in my skills and knowledge. Finally, a big thank goes to Raini for sustaining my heights and downs during that time with an incredible patience and supporting me in everything I do.

6. Curriculum vitae

Author:	**Sabine Mall**
Address:	21, Wimbergergasse, 1070 Vienna, Austria
Phone:	0043- 650/4790224
E-mail:	Sabine_Mall@gmx.at
Nationality:	Italy
Date of birth:	23.09.1985

Education

2004 – 2010	Studies in molecular biology Specializing in immunology, cell biology, and molecular medicine University of Vienna, Austria
1999 – 2004	Secondary school: Gymnasium 'Josef Ferrari' Merano, Italy
1991 – 1999	Primary school: Prad am Stilfserjoch, Italy

Practical experience

06.2009 -05.2010	Diploma thesis 'Assessment of therapeutic drug efficacy in the epithelial to mesenchymal transition of human liver cancer' A.o. Univ. Prof. Dr. Wolfgang Mikulits, Institute of Cancer Research, Medical University, Vienna, Austria
02.2009 -04.2009	Internship 'Differentiation of hepatic stellate cells, cloning of human stem cell factor' Dr. Tamás Schweighoffer, Novartis Institue of Biomedical Research, Basel, Switzerland
07.2008 – 09.2008	Internship 'Spheroid formation of liver tumor cells in the presence of hepatic myofibroblasts' A.o. Univ. Prof. Dr. Wolfgang Mikulits, Institute of Cancer Research, Medical University, Vienna, Austria
02.2008 - 04.2008	Internship 'The influence of pollen-related food allergens on human dendritic cells' A.o. Univ. Prof. Dr. Heimo Breiteneder, Institute of Pathophysiology, Medical University, Vienna, Austria